# Final Design Report

# Bi-directional Rotary Actuator

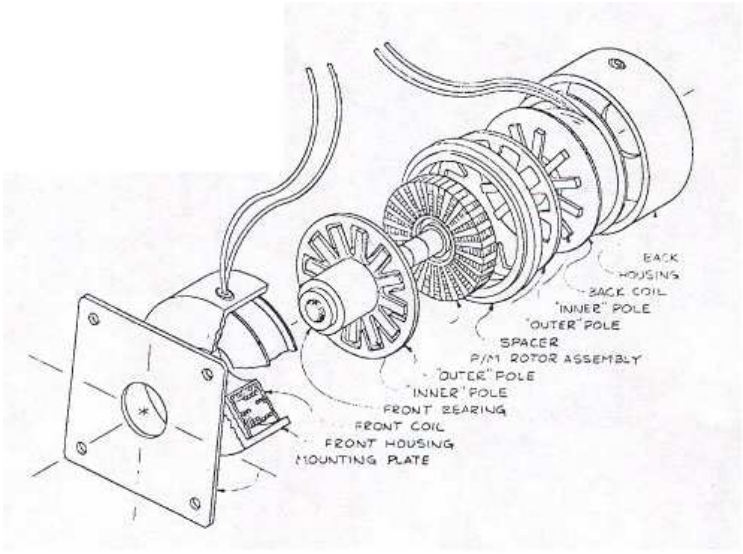


Sung Bae
Robert Hooge
Chris Imparato
Jose Jaramillo

Sponsored by:
Sandia National Laboratories
Sponsor:
Gilbert Benavides

December 3, 2007

# Table of Contents

# Appendices

# Executive Summary

The Compact Bi-directional Rotary Actuator project is sponsor by Sandia National Laboratories. This actuator project would be based on Micro-Electro-Mechanical Systems (MEMS) technology. However, the actuator prototype design and construction would be scale up do to lack of knowledge and access to the technology and for budget constraints. The model actuator is going to have 2 inches. Soon after the actuator prototype is conclude and approved, the Sandia Labs would scale it down to there specific needs. The desire application of this step motor design is to be part of a locking mechanism for an unspecified weapon system.

The step motor design had almost no room to play with. Our sponsor representative, Gilbert Benavides from Sandia National Laboratories, had specific needs for the motor. Such specifications were the used of one coil, a pancake style design, one set of outer poles, one set of inner poles, and a compact and easy to assemble housing, and a torque of 0.3 Nm. Other factors were left for the team and advisors to decide. For instance, dimensions, materials, air gaps, inside arrangements, and housing. Even though specifications are made, designing a mechanism involving such requirements it is not an easy task to reach because so many needs produce many limitations.

To reach the goals require by our sponsor, we had to utilize a computer simulation program call Maxwell 2D and 3D. The advisors for the project, Dr. Philippe Masson and Dr. Ongi Englander, were very helpful in guiding the team through these programs. The Maxwell software was used to determine how much current the coil needs, size of air gaps, position of magnets, and other specifications to achieve the necessary torque. Using Maxwell did only estimate answers, but it saves time, labor, funds, and defiantly takes the project in the right path. The latest model developed in Maxwell output the following results; using 1500 Amps turns torque result in 0.42141 Nm, while temperature reached 71.4 °C. Furthermore, the Bi-directional Rotary Actuator project is currently a computer and paper design only, which meets expectations for the time being. The project has enough data to proceeds with the fabrication and testing of a tangible mechanism.

## Section 1 - Introduction

The Bi-directional Rotary Actuator assigned by the Sandia National Laboratories for the senior design project is related to MEMS technology. This field is responsible for fabrication electro-mechanical system is a microscopic scale using integrated circuit process sequences. MENS' more commonly fabricated mechanisms are sensors and actuators. A pancake style actuator with one coil and a compact design is what the project final deliverable would be. An actuator or step motor is a mechanism that transforms electrical power in mechanical force. However, this type of motor are not in constant motion and do not need a brake system to stop them. These motors move in steps how their names highlights, and those distances are set according to each specific needs. Gilbert Benavides from Sandia Labs had a need assessment for the motor to rotate in steps of 25 degrees.

For the past three month our team has been working with one general design which had have small modifications specially in dimensions and material selection. Due to so many needs require by our sponsor the mechanism's esthetic cannot change much. After manipulating the idea on simulation software (Maxwell), our team has found that the torque of 0.3 Nm require to be reach is feasible. Also, calculation results explain that the actuator in operation would produce more than 70 degrees Celsius. Such temperature would require a heat transfer system to avoid any malfunction. Furthermore, our team looks forward to the fabrication period expecting a fair amount of accuracy from the software and calculations, but ready to tackle any difficulties.

## Section 2 - Problem Definition

This project is to design and fabricate a bi-directional rotary actuator for Sandia National Laboratory. The concept modifies an original design that has two coils and reduces it to one coil. The goal is to duplicate or improve the performance by using only one coil. This single coil will reduce the weight as well as the size of the overall device. If successful, the design will be scaled down to nano or micro size and used as a safety device for weapons.

## Section 3 - Background

It is necessary to understand the principles of magnetism and electromagnetic motors in order to understand how a bi-directional rotary actuator works. Magnetism is one of the peculiar physical characteristics, which is caused by acts of the attractive or repulsive forces within a magnetic field. Magnetic fields can be seen where magnetic forces of magnetic dipoles are detected. It also occurs by electrical currents through wires because those electrical currents affect the others, which is called electromagnetism. Specifically, the motion of electrons produces magnetic field because every electron has a magnetic attribute. Magnetic force is calculated by cross product of electric charge, velocity of charged element, and magnetic field; Fleming's left hand rule is applied to the force. In the rule, thumb, index finger, and middle finger indicate the direction of motion, field, and current respectively. The direction of the force is perpendicular to the magnetic field. Usually electromagnets are used for electromagnetism, which consists of a magnetic substance and coils wrapping around it. Iron, steel can be used as magnetic materials because magnets can attract those metals. When electric currents pass though the coils, the metal core is magnetized. The magnetized metal acts like a magnet, but the magnetic effect disappears when the current is not applied. The power of magnetic effect depends on the number of coils and the quantity of electrical current. By contrast, permanent magnets have magnetic attributes produced by the natural movement of electrons. Mainly mixtures of iron, cobalt, and nickel are used for permanent magnets.

In many fields, electromagnetism is used. An electric motor is one of the most important uses of magnets. It can switch electrical energy to mechanical energy. There are two types of electric motors: rotary and linear motors. The difference between two types of motors is the direction of movement based on how to assemble them. Also, an electrical motor can be classified by DC type and AC type. Among rotational actuators, a stepping motor has several advantages over other types of motors. It is able to position accurately because the degree per step of the rotary actuator can be controlled by the number of poles on a stator and permanent magnets on a rotor. Moreover, the rotary actuator can produce the highest torque at low speed. When currents are applied to a coil, poles on the stator are magnetized axially and magnetic field is formed. As magnetized poles act as electromagnets, they are in alignment with the opposite

poles of the permanent magnet on the rotor by attracting them and repelling the same poles of the permanent magnet on the rotor. This procedure makes the rotor rotate in one direction with a specific angle. By the opposite direction of the current applied to the coil, the rotor will rotate in the other direction.

# Section 4 – Design and Analysis

## 4.1 Concept Generation and Selection

Our design is based on the principles of an axial flux electric motor. When a current- carrying conductor is placed in a magnetic field, it is subjected to electromagnetic force or Lorentz force. This force is fundamentally important because it is the foundation of the motor operation. The magnitude of this force depends on orientation of the conductors with respect to the magnetic field. The force is at its maximum when the conductor is perpendicular to the magnetic field and becomes zero when it is parallel.

### 4.1.1 Design 1

This design calls for the use of one coil to operate the rotor. The single coil allows the actuator to be very small and lightweight. The design is considered a pancake style design because the coil will be directly above the rotor not surrounding the rotor. The direction of the rotor is controlled by the direction of the current flowing through the coil. For example if the current flows left to right, then the rotor rotates clockwise and vice versa. When the coil has no current flowing through it, then the rotor will return to its neutral position. This actuator will rotate both clockwise and counterclockwise approximately 22.5º. For an actuator of a certain size, it takes advantage of the rotors maximum moment arm. This means that the radius of the rotor is its maximum given the radius of the entire actuator. This design contains a mounting plate, an outer housing, an inner pole, an outer pole, a coil, and a permanent magnet rotor.

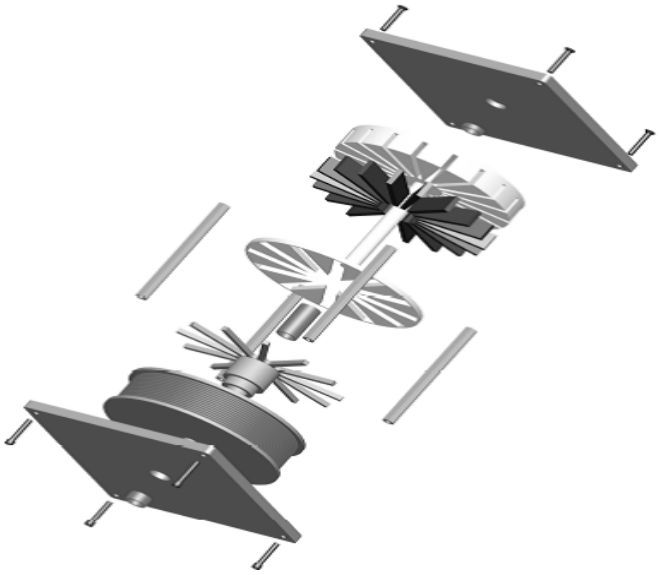

Figure 4.2-1 – Original actuator design

Although this design was worked in principle many of its components were too complex to manufacture with the time and resources of this project in mind. The stators alone would have to be made of 10-20 separate pieces of iron and then a way of connecting these pieces would have to be created.

### 4.1.2 Design 2

This design is very similar to the first design only this design uses two coils instead of one coil. The two coil design is larger and it weighs more. This design is also pancake style. This design includes everything in design one with an extra coil and inner and outer poles.

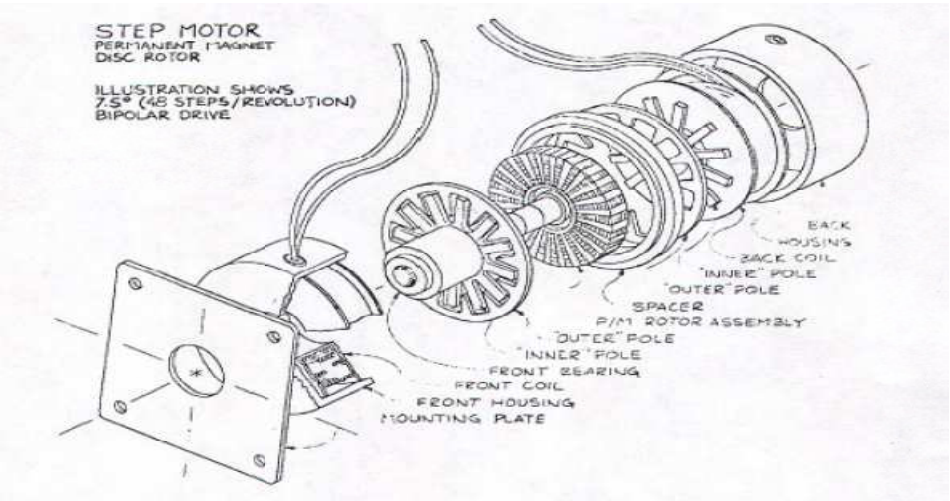


Figure 4.2-2 – Basis for actuator design

The advantages of the disk-rotor permanent magnet motor with 2 coils are that first the motor diameter can be made smaller than a conventional cylindrical- rotor motor having similar performance characteristics. At the same time since the poles on the rotor are magnetized in the axial direction, oriented magnetic materials may be used instead of the non-oriented materials. The oriented materials have a greater flux density which produces more torque per ampere of input current than a non-oriented material. As a result, the motor efficiency is improved. Below is a diagram of the actuator's operation principal.

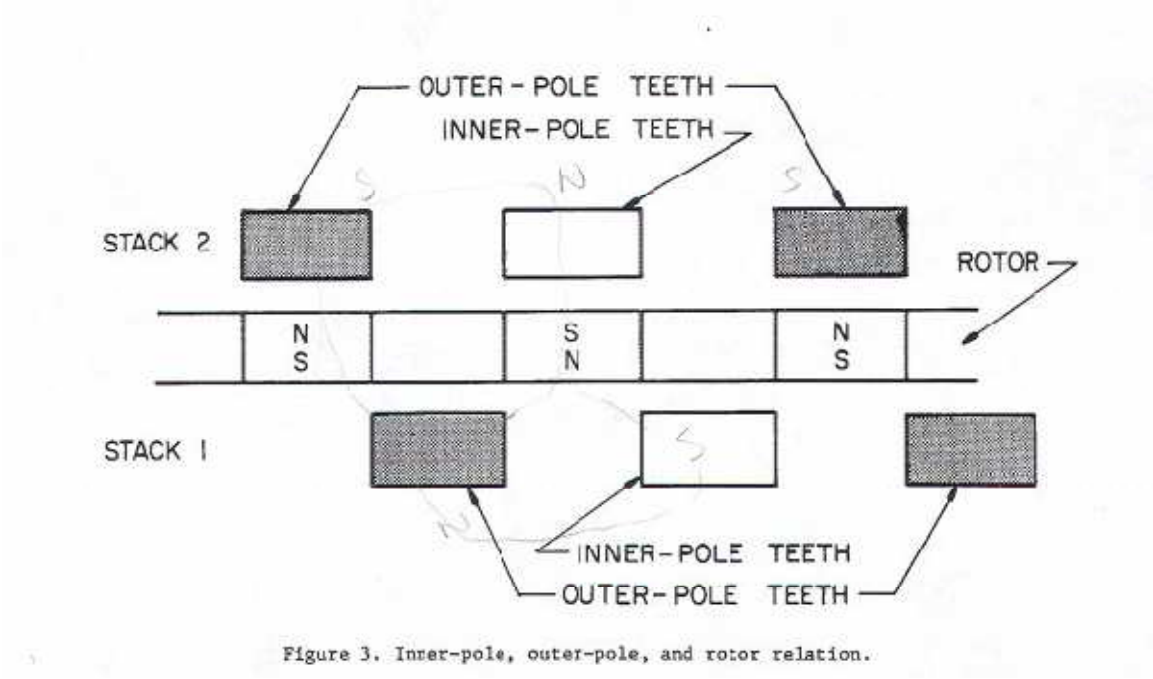

Figure 3. Inner-pole, outer-pole, and rotor relation.

Figure 4.2-3 – Operation of 2 stator actuator

When the teeth of stack No.1 of the stator are in alignment with the rotor poles, those of Stack No.2 are in total misalignment. Thus, as the phase energization is switched from Stack 2 to Stack 1, the rotor will rotate one-half of a pole pitch of the rotor. For example, if Stack 2 is polarized to S, N, and S, the rotor remains stationary. After that, the teeth of the rotor rotate to align with the Stack 1 when Stack 1 has polarization with N, S, and N.

### 4.1.3 Design 3

This design contains one coil in which that coil surrounds the rotor. These actuators are currently designed by many different companies. The functionality is the same as the above two designs the coil and rotor are just in different orientations. This design however, does not take

advantage of the maximum moment arm. The rotor radius is smaller than the actuators radius making the moment not as large as it can be for an actuator of that size.

The advantages of this design are that it dissipates much less power in losses such as heat than the cylindrical rotor and that it produces high torque and speed for its size. The main disadvantage to this type of actuator is that it produces a smaller torque than the 2-coil type because the surrounding coil constrains the size of rotor disk. The diagram below show how this style actuator works.

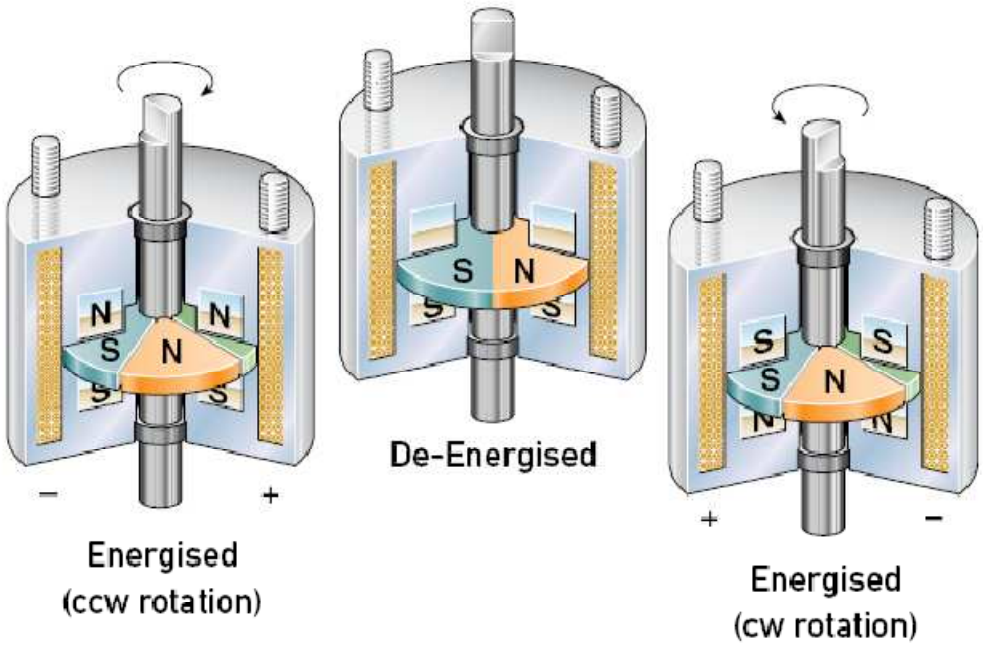


Figure 4.2-4 – Operation of single coil surrounding rotor

In the de-energized state, the armature poles each share half a stator pole, causing the shaft to seek mid-stroke. When power is applied, the stator poles are polarized. This attracts half and repels the other half of the armature poles, causing the shaft to rotate. When the voltage is reversed, the stator poles are polarized with the opposite pole. Consequently, the opposite poles of the armature are attracted and repelled, thus causing rotation in the opposite direction.

### 4.1.4 Final Design

Our final design uses one coil and two stators to apply force to the rotor. This design is by far the most compact and simple of the group, but sacrifices torque to achieve these qualities. Because of the strict requirements of our project this design is the

most desirable of all the designs. Even though the torque is lower than the previous design it is still within our performance specifications.

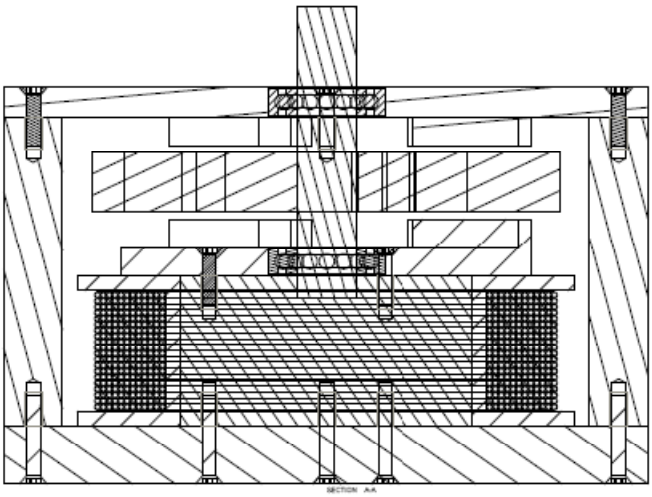

Figure 4.2-5 – Final design cross sectional view

This actuator design uses principles from all of the above designs. Although it is single coil design, the outer housing is made of a magnetic material so the lower pole of the coil can be channeled to the upper stator. This effect acts as a second coil, but in order to achieve this, the current through the coil must be greater than if there actually were two coils. The operations and specifications of this design will be discussed in the following sections and appendices.

## 4.2 2D Modeling and Analysis

### 4.2.1 Maxwell 2-D Model

All of the 2-D modeling was done in Maxwell SV. Maxwell SV is the leading electromagnetic simulation software program that delivers numerical power and ease of use for analyzing electrostatic and magneto-static designs. This 2-D model was constructed after researching the principles of rotary actuators and stepper motors. First a hand sketch was done during a teleconference with our sponsor. Once the initial dimensions were agreed upon, the model was created using simple shaped to represent the real world actuator. The software contains the material properties to determine how a magnetic field will effect and translate through the model; therefore each component must be assigned a material. Then, inputs and boundary conditions were established. In order to establish the flow of the current, a current source was placed in both sides of the coil. These two current sources had opposite signs indicating the direction the current was to flow. The magnetic field generated by the flowing current interacted with the surrounding materials and caused the magnets to move depending on the direction of the current. Next the executive parameter was set up. In this case the force generated between the magnets and the stators was measured. This force could then be taken and multiplied by the radius of the rotor to obtain the theoretical torque (See Appendix A). Finally, a solution had to be determined. Once a solution was converged upon, post processing graphs and output variables could be displayed.

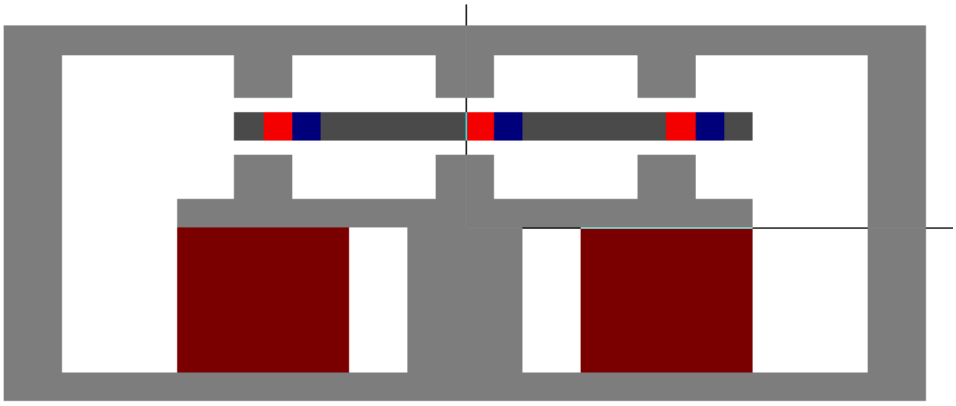

**Figure 4.2-6 – 2D model of rotary actuator**

### 4.2.2 Maxwell 2-D Analysis

Figure 4.2-7a and 4.2-7b show the magnitude of the magnetic field and the direction of the magnetic flux lines respectively. This is useful in determining the gaps between the components of the actuator. As can be seen in the figures below, no parts of the actuator have become magnetically saturated; this indicates that the gaps in our final design were sufficient.

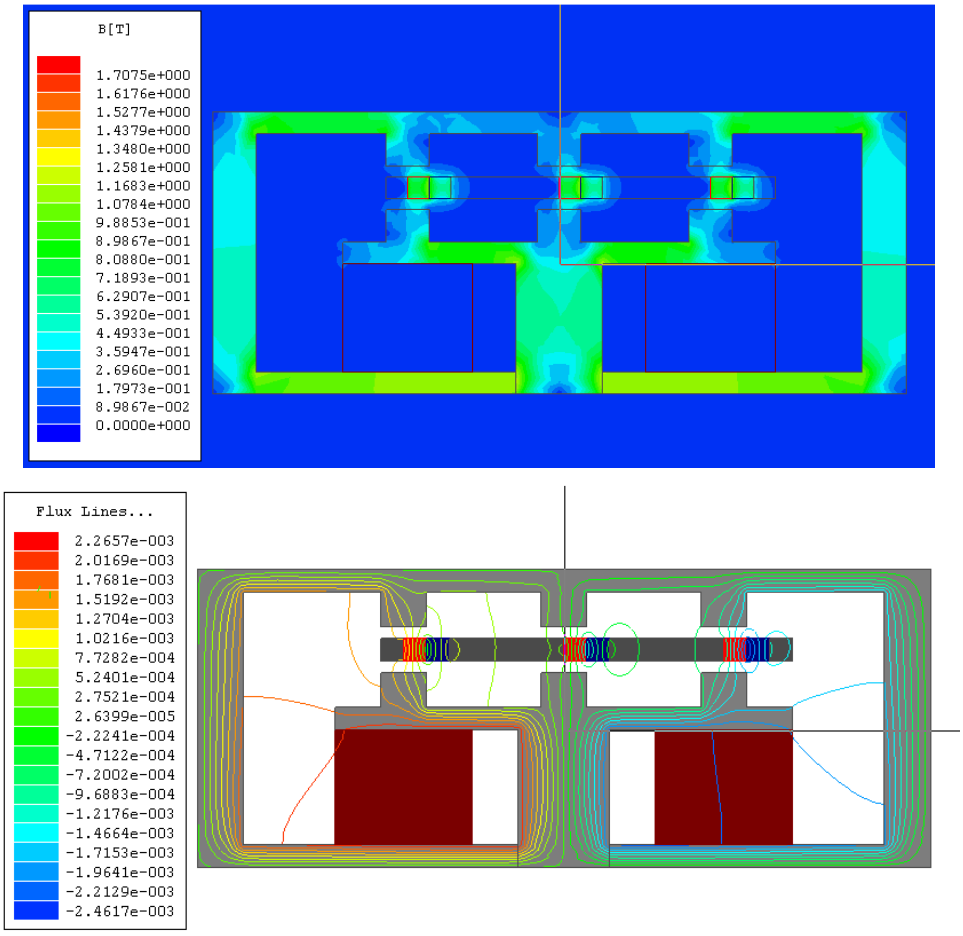


Figure 4.2-7a: (top) Magnetic field magnitude plotted on surface.

Figure 4.2-7b: (bottom) Magnetic flux lines plotted on surface

## 4.3 3D Modeling and Analysis

### 4.3.1 Maxwell 3-D Model

The 3-D modeling was all done in Maxwell 3-D. Maxwell 3-D is a finite element software used for analyzing electrostatic and magneto-static designs. A 2-D model was first constructed and analyzed to use as a starting point for dimensions and other variables. Certain dimensions had to be altered significantly because the equations and variables are very different from 2-D to 3-D. Once the 3-D model was constructed, materials were assigned to the different parts. The software contains the material properties to determine how a magnetic field will effect and translate through the model. Then, excitations and boundary conditions were established. A current was placed through the copper coil inducing a magnetic field. This magnetic field interacted with the surrounding materials and caused the magnets to move depending on the direction of the current. Next the executive parameter was set up. In this case the torque of the rotor was calculated by the software because the calculations would be too difficult to do by hand. Finally, a solution had to be determined. The number of passes the software should make and the percent of error acceptable for a solution were input. Once a solution was converged upon, post processing graphs and output variables could be displayed.

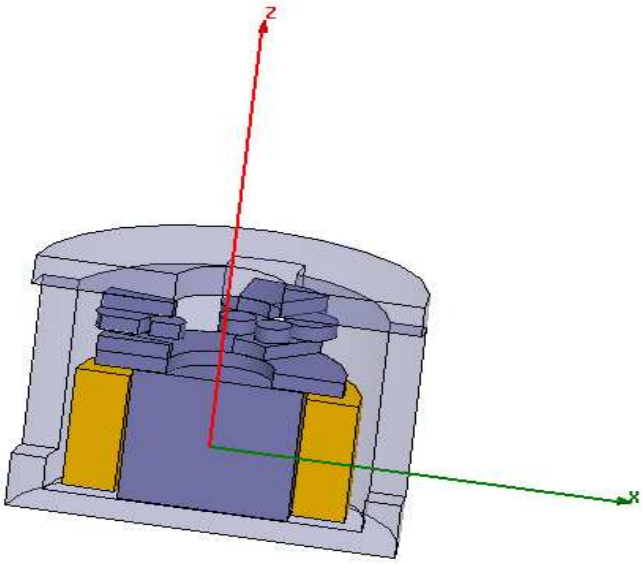


Figure 4.3-1: Cross Section of 3-D Model

### 4.3.2 Maxwell 3-D Analysis

Figure 4.3-2a and 4.3-2b show the magnitude of the magnetic flux in the various parts. This is useful in determining whether or not the field created by the coil will saturate any of the steel which would decrease the performance of the actuator. The graph shows that no piece of the actuator is saturated and should be working at peak performance.

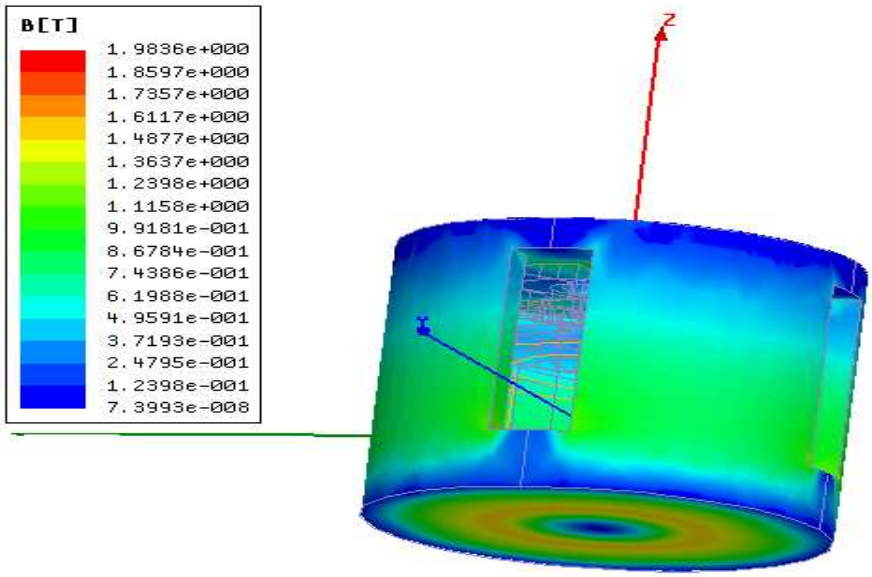


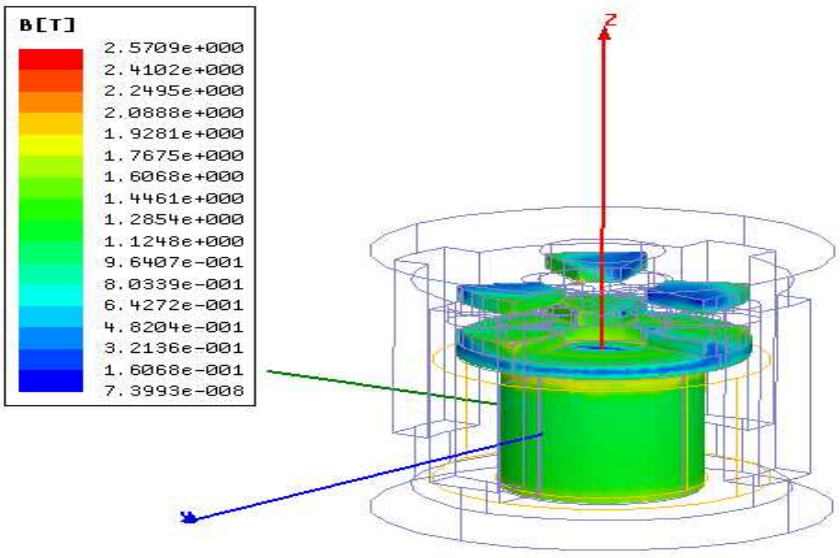


Figure 4.3-2a: (top) Outer housing magnetic flux plotted on surface.

Figure 4.3-2b: (bottom) Inner parts magnetic flux plotted on surface

This graph shows the vector lines for the magnetic field. As they show, the field lines start from the core of the coil and then disperse up the actuator and circle back around to the coil proving the design is functional.

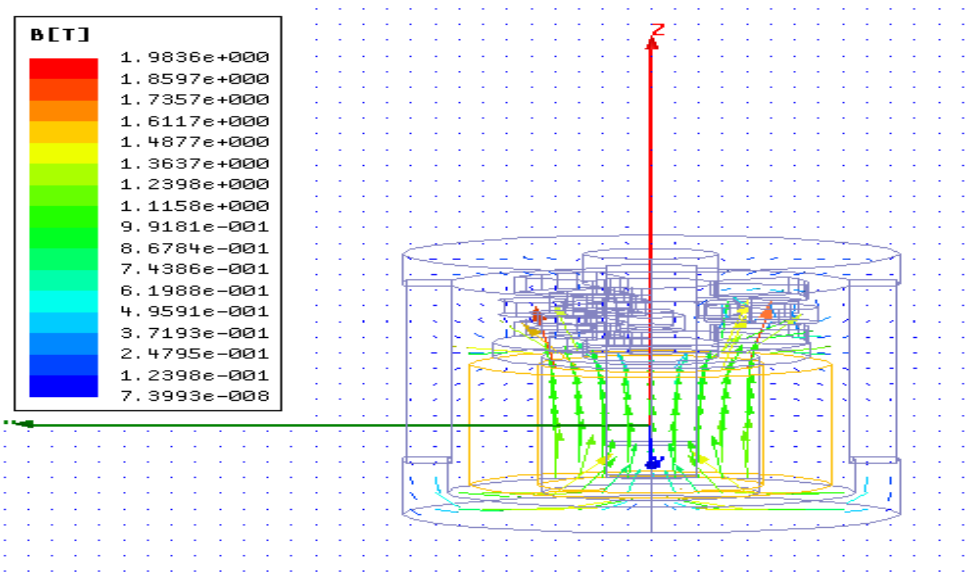


Figure 4.3-4: Magnetic field lines in actuator

### 4.3.3 Thermal analysis on E-Physics

E-physics is a finite element software package that can determine thermal characteristics of systems. This program worked well with our design because importing the design was easy and the software is based like Maxwell 3-D. Thermal analysis is needed because the surface temperature of the actuator needs to be determined. The graph below shows the temperature distribution over the surface of the actuator. This surface temperature is important because this is the temperature that will actually be felt by other components around the actuator. The temperature distribution will be when the actuator is at steady state so these values are relatively conservative. The actual temperature might not reach the values in the picture. To also be on the safe side, four fans will be used to remove some of the heat out of the system.

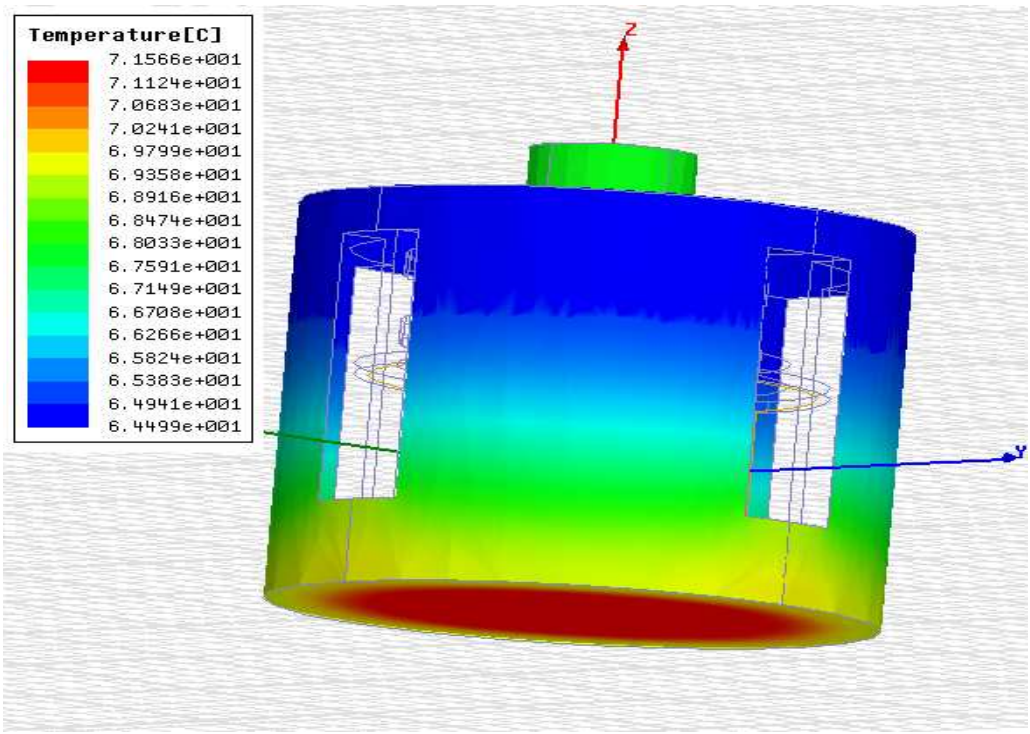


Figure 4.3-5 Temperature distribution on surface of actuator.

### 4.3.4 Optimization

The main size constraint for this project was to keep the rotor at a 2 inch diameter. This left many different parameters to be optimized to reach the desired torque of .3Nm. The effect of changing a single parameter would affect the rest of the design. For instance, if the air gap was decreased to increase the magnetic field felt by the magnets, the attraction between the magnets and the stator would increase as well and that attraction must be overcome before the rotor would move. Each individual parameter was taken separately and the effects on the system were simulated. If a low torque was encountered more amp turns were added to increase the magnetic field. The higher amp turns account for higher temperatures that could potentially be hazardous if the amp turns get to high. The increase in amp turns would also increase the magnetic field that would be measured on the surfaces of the materials to determine if the material becomes saturated. If saturation occurred, the amp turns would be decreased and the magnets would be moved closer to the stators. As stated before the smaller the air gap the more torque the rotor has to overcome. Also the magnets have a strong magnetic field which

increases as the distance between decreases. This could possibly saturate the stator and the system would become useless.

There also was a problem of where to line the magnets up in a starting position. The goal was to find the position that would generate the greatest initial torque. Simulations were run at various orientations and the torque was calculated. The position with the greatest torque was when the middle of the magnets were over the sides of the stators.

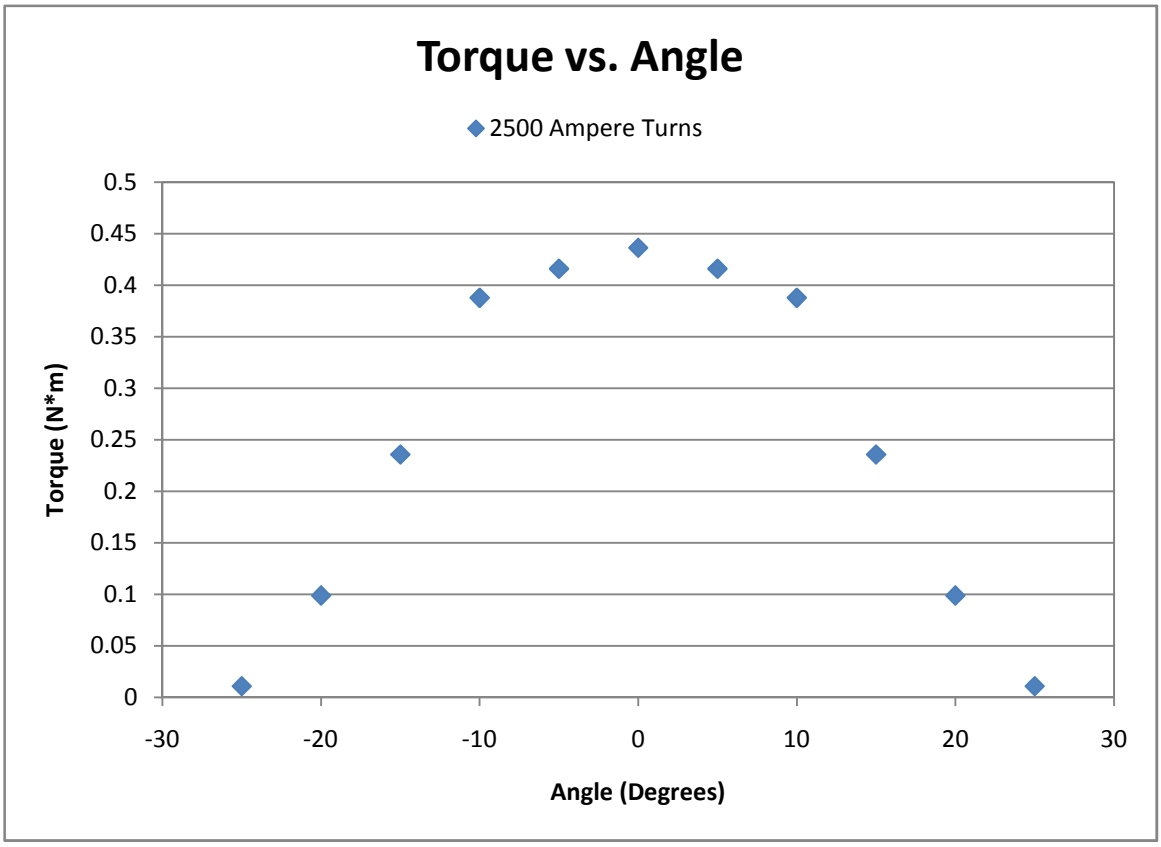


Figure 4.3-6 Torque vs. magnet angle

Figure 4.3-6 shows when a positive or negative voltage is applied it causes the shaft to rotate clockwise or counterclockwise. When the power is removed, the restoring torque brings it back to a neutral position. The torque decreases as the rotor turns farther because the magnets reach an equilibrium position and will no longer move. This occurs at about 30°.

## 4.4 Prototype

The prototype was modeled in Pro/E Wildfire 3.0 in order to have drawings for machining the prototype (Appendix E). Below is the Pro/E assembly as well as the exploded view of the Actuator model. Once all of the simulations were complete it was decided upon that due to thermal concerns the current in our design would be limited to 1500 ampere turns. Although this put a limit on our torque as well we were still able to achieve our goals and produce a torque of 0.41 Nm (Our goal was a torque of 0.31 N*m, see Appendix F, section II).

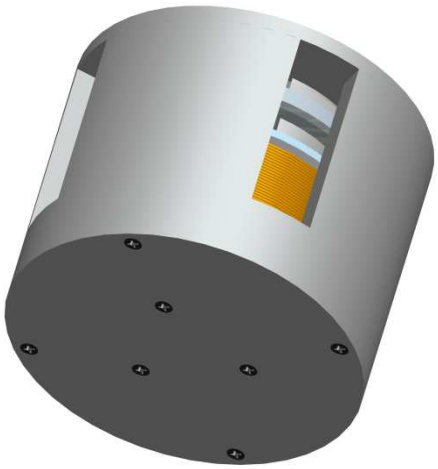

Figure 4.4-1 – Actuator model assembly

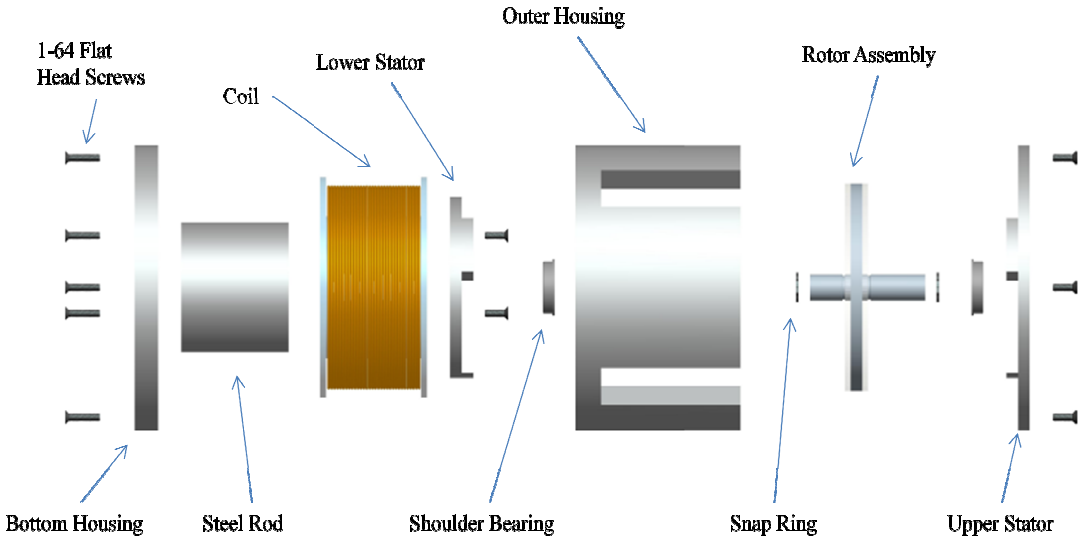


Figure 4.4-2 – Actuator model exploded view

## 4.5 Materials Selection

For the most part the materials to be used were specified by the sponsor and can be reviewed in Appendix C. These materials were used in Maxwell 2D and 3D as close as possible. Equivalent materials were chosen for materials that were not available in the software.

The housing of the model is made of Steel 1045 in order to conduct the magnetic fields from the coil. The material acquired for the rest of motor components was as specified by the sponsor, but the shape of some components is different from the original reference motor. The shape was changed from square to round in order to more uniformly conduct the magnetic field, this results in more torque. Disc shaped NdFeB magnets are used and after many trials with the Maxwell software it was determined that we will use a mixture of 0.375 and 0.25 diameter magnets. Both sizes of magnet are 0.125" thick and six of each size will be embedded inside of an aluminum rotor.

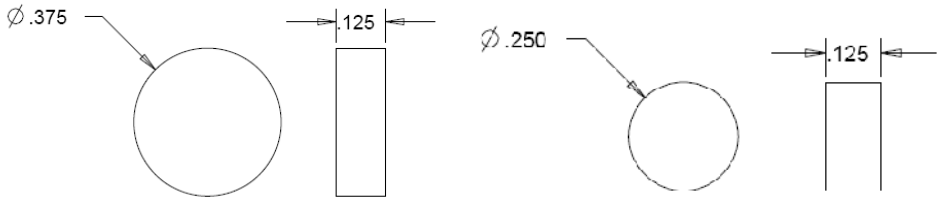


Figure 4.5-1 – Dimensions of NdFeB Magnets in system

# Appendix A

# Calculations

## 2D Force and Torque Calculations

The radius of the rotor $r := 1in$

Force given by Maxwell software $F := 16.995N$

The torque can be estimated by $\tau := F \cdot r$

Estimated torque $\tau = 0.432\,N \cdot m$

## Wire Diameter and Length

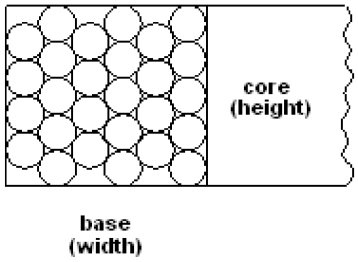


$ID := 1.25in$ $OD := 2in$ $h := 1in$

$w := \frac{OD}{2} - \frac{ID}{2}$ $w = 0.375\,in$

$A_{cross} := w \cdot h$ $A_{cross} = 0.375\,in^2$

$D_{wire} := \frac{h}{40}$ $D_{wire} = 0.025\,in$

A 22AWG wire has a diameter of 0.254in, this is close enough to our calculated diameter

Number of turns $N_{turns} := 504$

$L(t) := \lceil 2 \cdot \pi \cdot (0.70 + 0.0251 \cdot t) \rceil in$

$L := 40 \cdot (L(0) + L(1) + L(2) + L(3) + L(4) + L(5) + L(6) + L(7) + L(8) + L(9) + L(10) + L(11) + L($

$L = 2.779 \times 10^3\,in$

$L = 231.594\,ft$

The length of copper wire that we will need is 232ft

$A_{wire} := \pi \cdot \left( \frac{D_{wire}}{2} \right)^2$ $A_{wire} = 4.909 \times 10^{-4}\,in^2$

$\rho_{copper} := 0.322 \frac{lb}{in^3}$

$V_{wire} := A_{wire} \cdot L$ $V_{wire} = 1.364\,in^3$

$mass_{wire} := V_{wire} \cdot \rho_{copper}$ $mass_{wire} = 0.199\ kg$

$weight_{wire} := mass_{wire} \cdot g$ $weight_{wire} = 0.439\,lbf$

The wire used in our system will weigh 0.439 lbs

## Current Density and Power Supply Requirements

Current in the coil (Ampere turns) $I_{coil} := 1500A$

Resistivity of Copper $\rho := 1.67 \cdot 10^{-8} \Omega \cdot m$

Current Density is given by $J := \frac{I_{coil}}{A_{cross}}$ $J = 6.2 \frac{A}{mm^2}$

A current density above 5 indicates that activate cooling is needed. This is an acceptable solution up to 10.

Resistance of wire $R := \frac{\rho \cdot L}{A_{wire}}$ $R = 3.722\ \Omega$

Power Supply current required $I_{supply} := \frac{J \cdot A_{wire}}{\frac{\pi}{4}}$ $I_{supply} = 2.5\ A$

Power Supply voltage required $V := I_{supply} \cdot R$ $V = 9.306\ V$

Heat Generated by Coil $P := I_{supply}^2 \cdot R$ $P = 23.265\ W$

## 3D Torque Calculations

Number of turns $N_{turns} := 504$

Air gap between stator and magnets $d := 0.3125in$

Permeability of Air $\mu_o := 4 \cdot \pi \cdot 10^{-7} \frac{T \cdot m}{A}$

Permeability of Iron $K_{m\_iron} := 0.377$

$\mu := K_{m\_iron} \cdot \mu_o$ $\mu = 4.738 \times 10^{-7} \frac{kg \cdot m}{s^2 \cdot A^2}$

Using the magnetic flux equations and force equations we can estimate the 3D torque using the following formula $\tau := r \cdot \mu \cdot N_{turns} \cdot \frac{I_{supply}^2}{d} \cdot 2 \cdot L$

The estimated torque is $\tau = 0.674\,N \cdot m$

This Torque is slightly higher than what we were able to achieve in our 3D simulations. I
real world conditions that are not taken into account by the above equations, the torque gi
is ideal.

# Appendix B

# Graphs

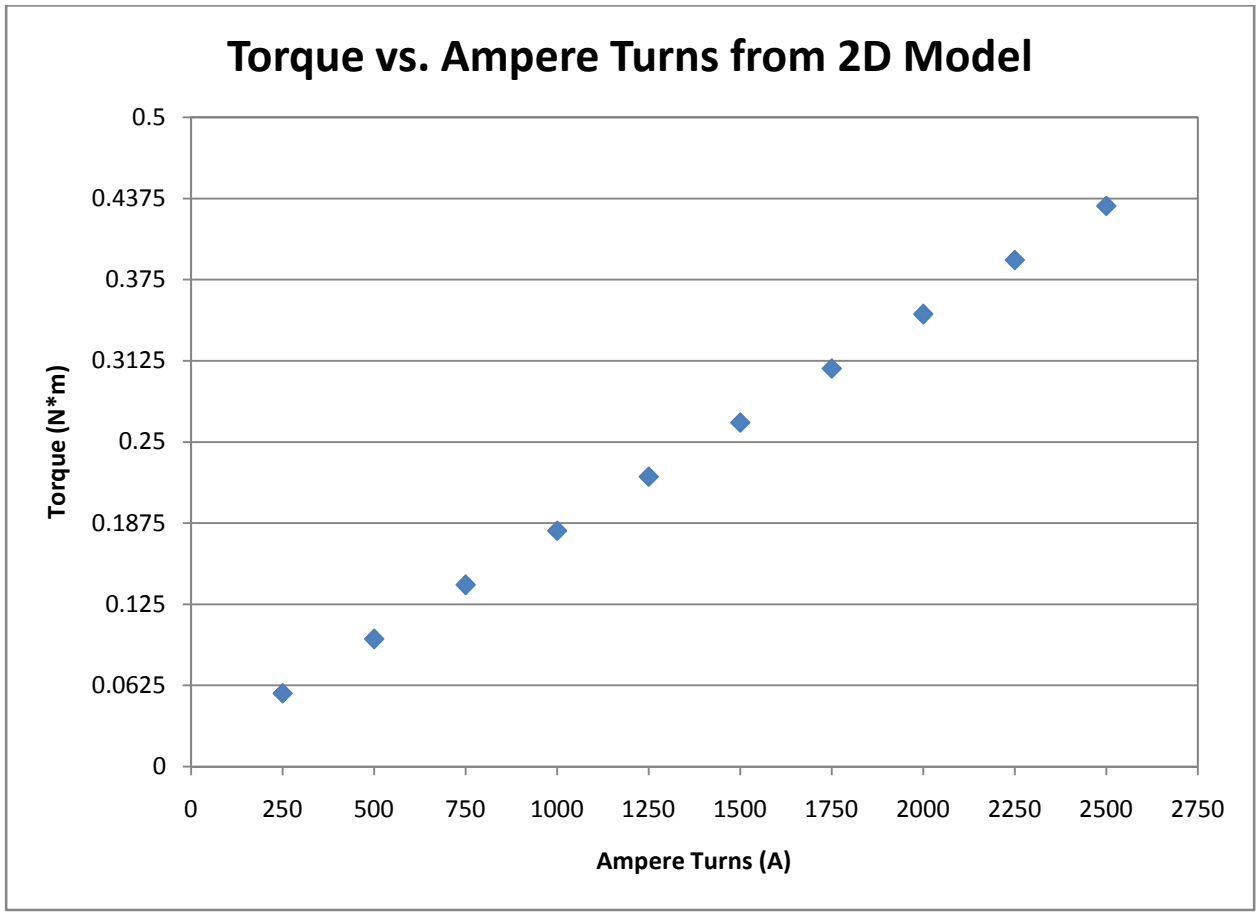


The graph above shows how the torque between the magnets and the stators changes as the total current in the coil is increased. This graph was created using data gathered from a Maxwell 2D simulation of our final design. All of the parameters were held constant except for the current in the coil. Although the torque increases with the current there will come a point where the entire device will become magnetically saturated and the torque begin to drop off and eventually go to zero.

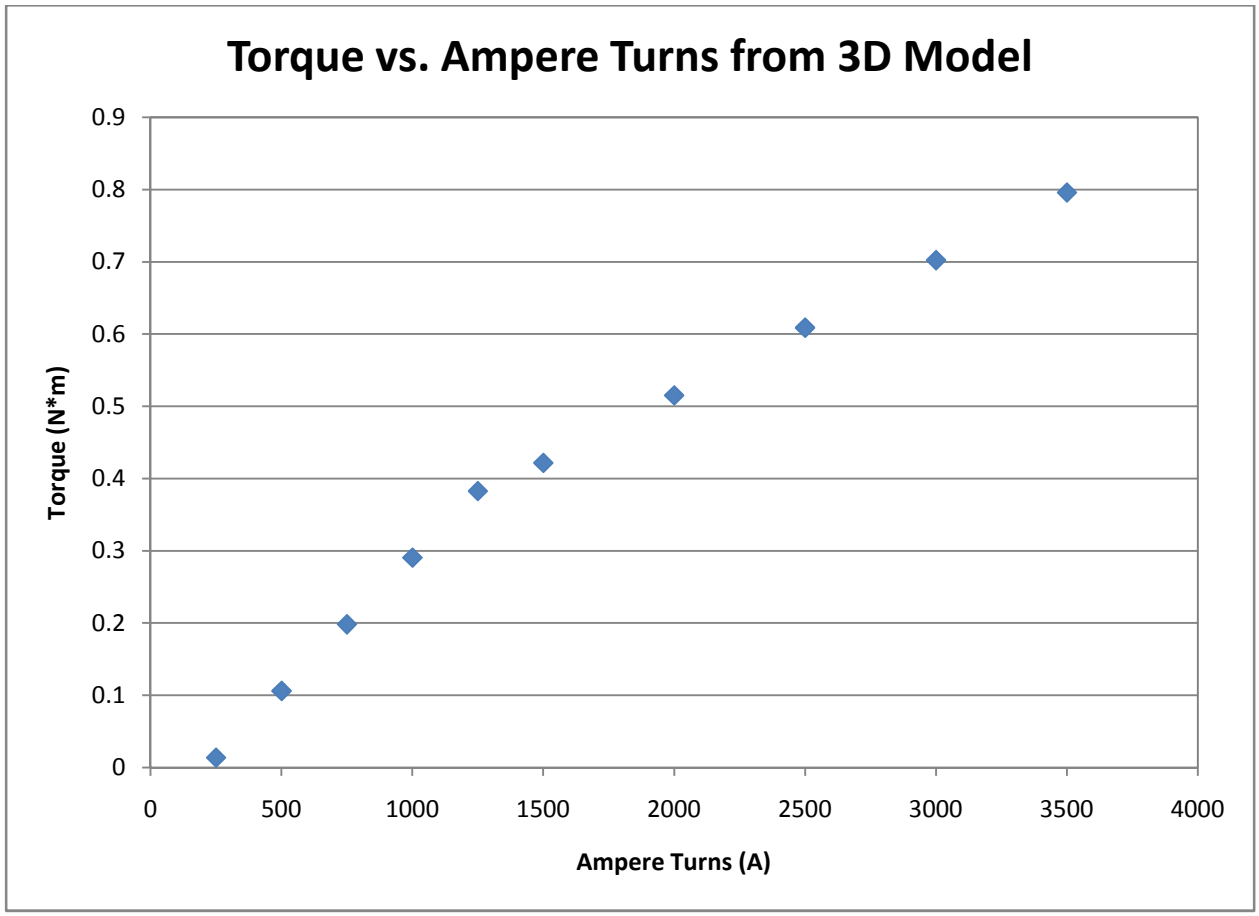


The graph above shows how the torque between the magnets and the stators changes as the total current in the coil is increased. This graph was created using data gathered from a Maxwell 3D simulation of our final design. All of the parameters were held constant except for the current in the coil. Although the torque increases with the current there will come a point where the entire device will become magnetically saturated and the torque begin to drop off and eventually go to zero. As you can see this graph is slightly different than the one above, in the 3D simulation the round shape of our device is taken into account which changes the magnetic flux throughout the housing of the actuator. This change in magnetic flux results in a slight difference in the calculated torque.

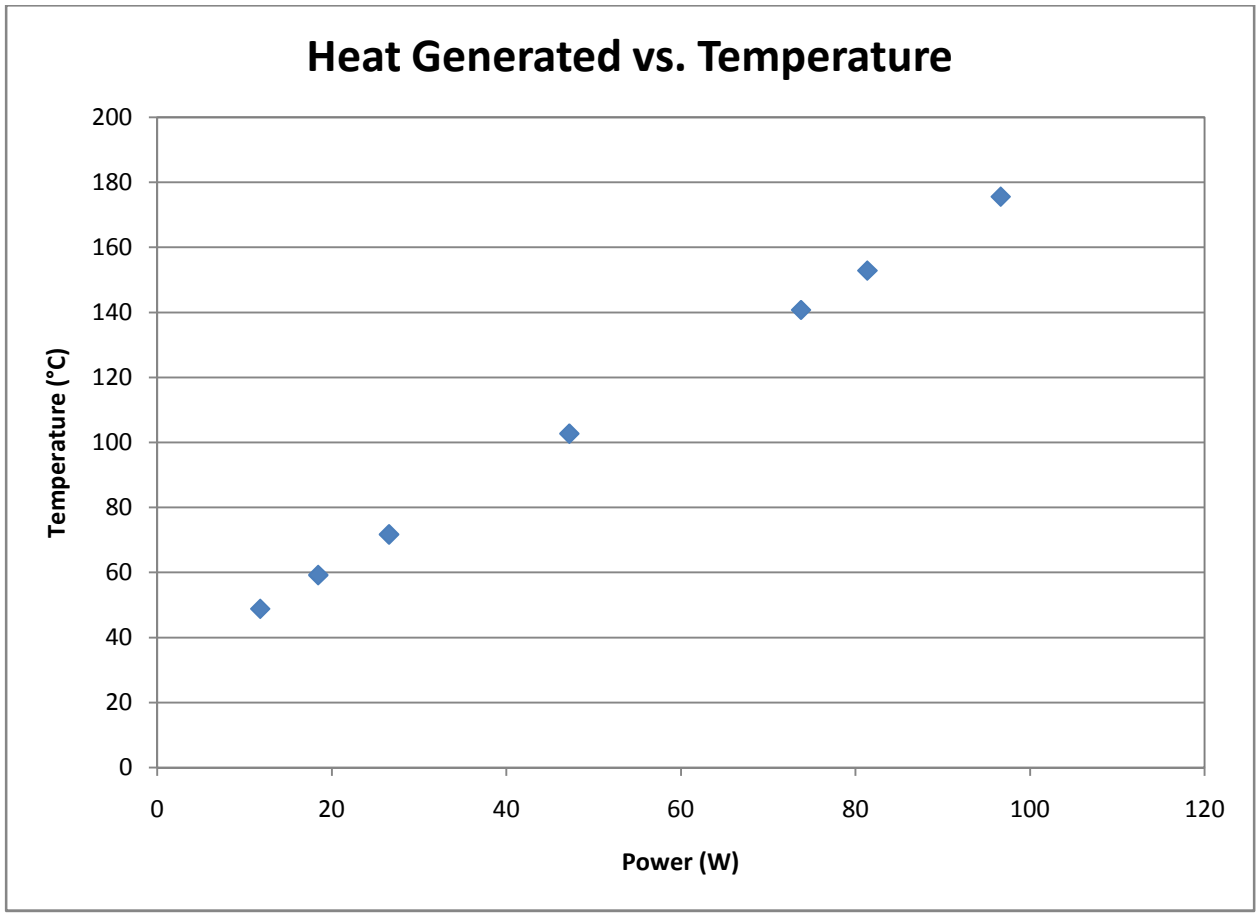


This graph shows how the surface temperature of the housing of the actuator changes with respect to the heat generated by the coil. Ideal thermal assumptions were made in order to simulate these temperatures, also much of the actuator's internal geometry was simplified in order to simulate using the available software. To create this graph we imported our 3D model from Maxwell into E-Physics and them using the calculations from Appendix A changed the heat generated by the coil according to the coil current. As the current density within the coil increases as does the heat generated and thus the temperature of the housing.

# Appendix C

# Materials

| Part | Material | Magnetic Properties | Thermal Properties | | Electrical Properties | Density ($kg/m^3$) |
|---|---|---|---|---|---|---|
| | | Curie Temperature (°C) | Thermal Conductivity (W/m*K) | CTE (µm/m*°C) | Electrical Resistivity (Ω*m) | |
| Housing | Steel 1045 | 1043 | 51.9 | 13.15 | 1.62E-07 | 7870 |
| Stators | | | | | | |
| Rod | | | | | | |
| Coil | Cu | - | 385 | 20.6 | 1.70E-08 | 8960 |
| Magnets | NdFeB | 310 | 2.931 | 3.4 | 0.00016 | 7650 |
| Rotor | Polyetherimide | - | 0.376 | 55.6 | 1.98E+14 | 1315 |

# Appendix D

# Diagrams

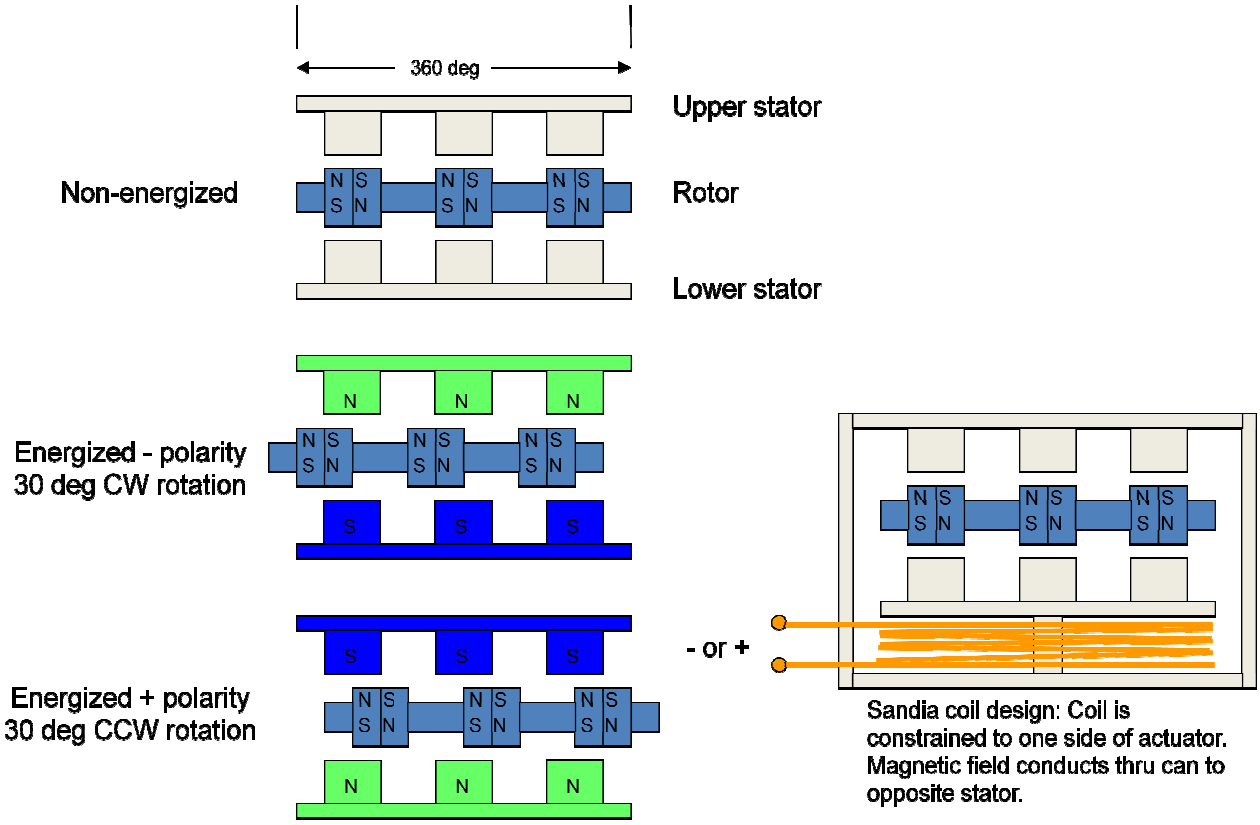


**The diagram above illustrates the operation of our final design. When the actuator is not energized the rotor is in a neutral position. Depending on what polarity the stator are magnetized in, the rotor will move to a new position.**

# Appendix E

# Pro Engineer Drawings

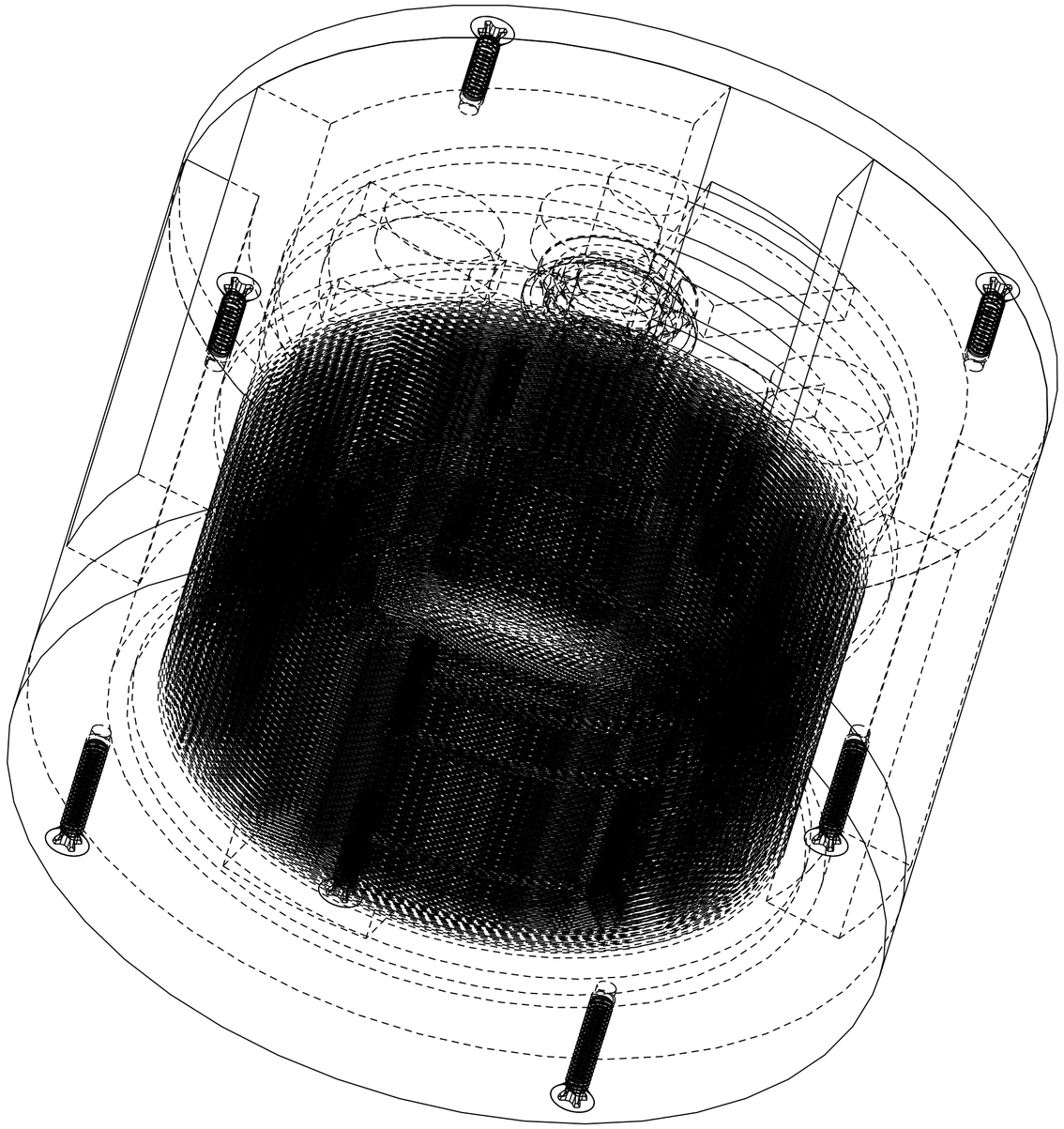

SCALE 3.000

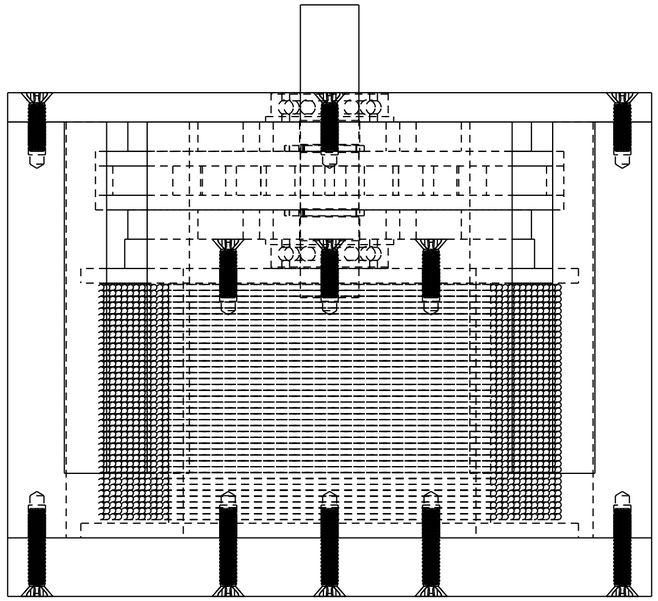

SCALE 2.000

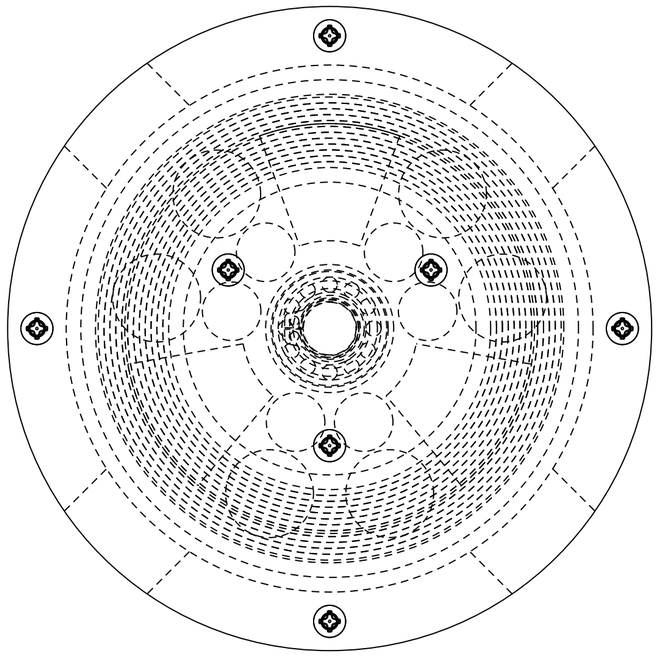

| | |
|---|---|
| Part: | Rotary Actuator |
| Project: | Rotary Actuator |
| Drawn by: | Group 9 |
| Date: | 11/30/2007 |
| Sheet: | 1 of 16 |
| Sandia National Laboratory | |
| FAMU-FSU College of Engineering | |

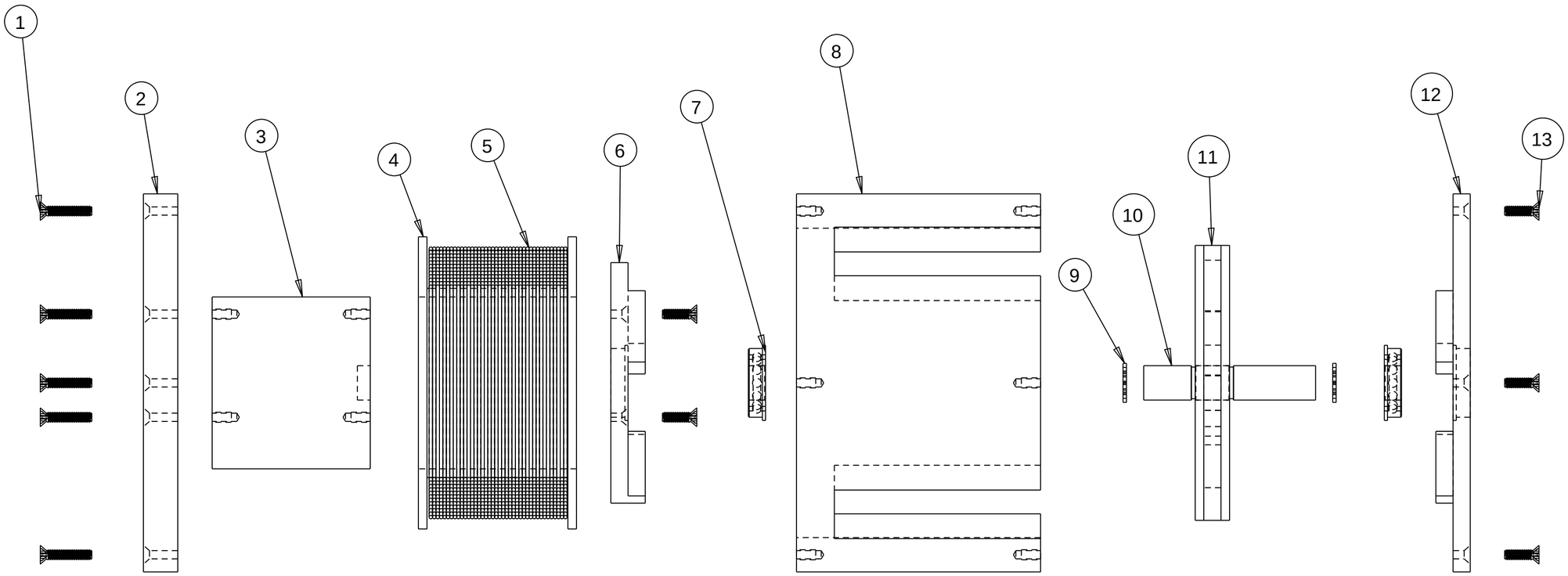


| | |
|---|---|
| Part: | Exploded View |
| Project: | Rotary Actuator |
| Drawn by: | Group 9 |
| Date: | 11/30/2007 |
| Sheet: | 2 of 16 |
| Sandia National Laboratory | |
| FAMU-FSU College of Engineering | |

SCALE 1.500

Bill of Materials:

| Quantity | Part # | Name |
|---|---|---|
| 7 | 1 | 1-64 FLAT HEAD SCREW .375 |
| 1 | 2 | BOTTOM HOUSING |
| 1 | 3 | STEEL ROD |
| 1 | 4 | COIL SPOOL |
| 1 | 5 | COPPER COIL |
| 1 | 6 | LOWER STATOR |
| 2 | 7 | SHOULDER BEARING |
| 1 | 8 | OUTER STRUCTURE |
| 2 | 9 | SNAP RING |
| 1 | 10 | SHAFT |
| 1 | 11 | ROTOR ASSEMBLY |
| 1 | 12 | UPPER STATOR |
| 7 | 13 | 1-64 FLAT HEAD SCREW .250 |

| | |
|---|---|
| Part: | Bill of Materials |
| Project: | Rotary Actuator |
| Drawn by: | Group 9 |
| Date: | 11/30/2007 |
| Sheet: | 3 of 16 |
| Sandia National Laboratory | |
| FAMU-FSU College of Engineering | |

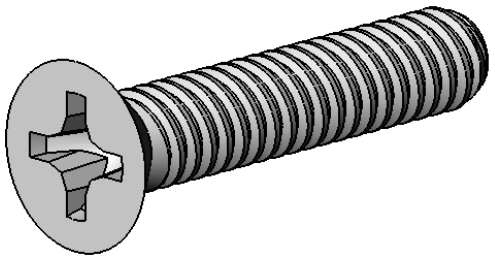

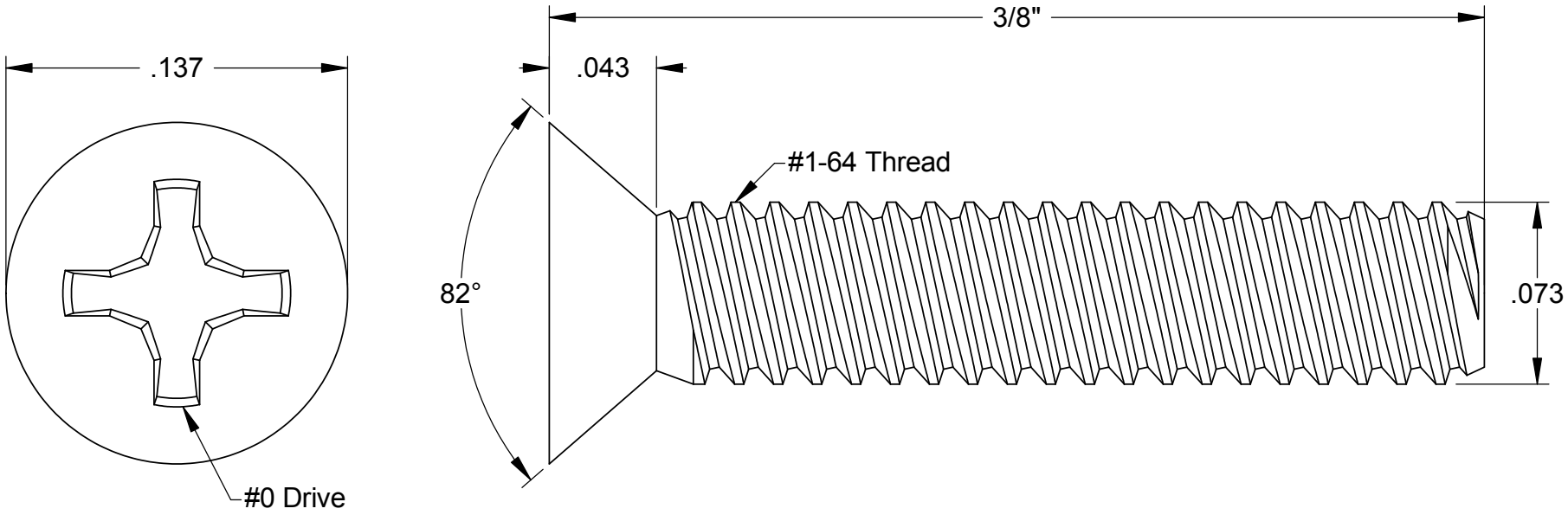


| | |
|---|---|
| McMASTER-CARR CAD | PART NUMBER **91771A068** |
| http://www.mcmaster.com<br>© 2005 McMaster-Carr Supply Company | 18-8 Stainless Steel Phillips Flat Head Machine Screw |

Unless otherwise specified, dimensions are in inches. Information in this drawing is provided for reference only.

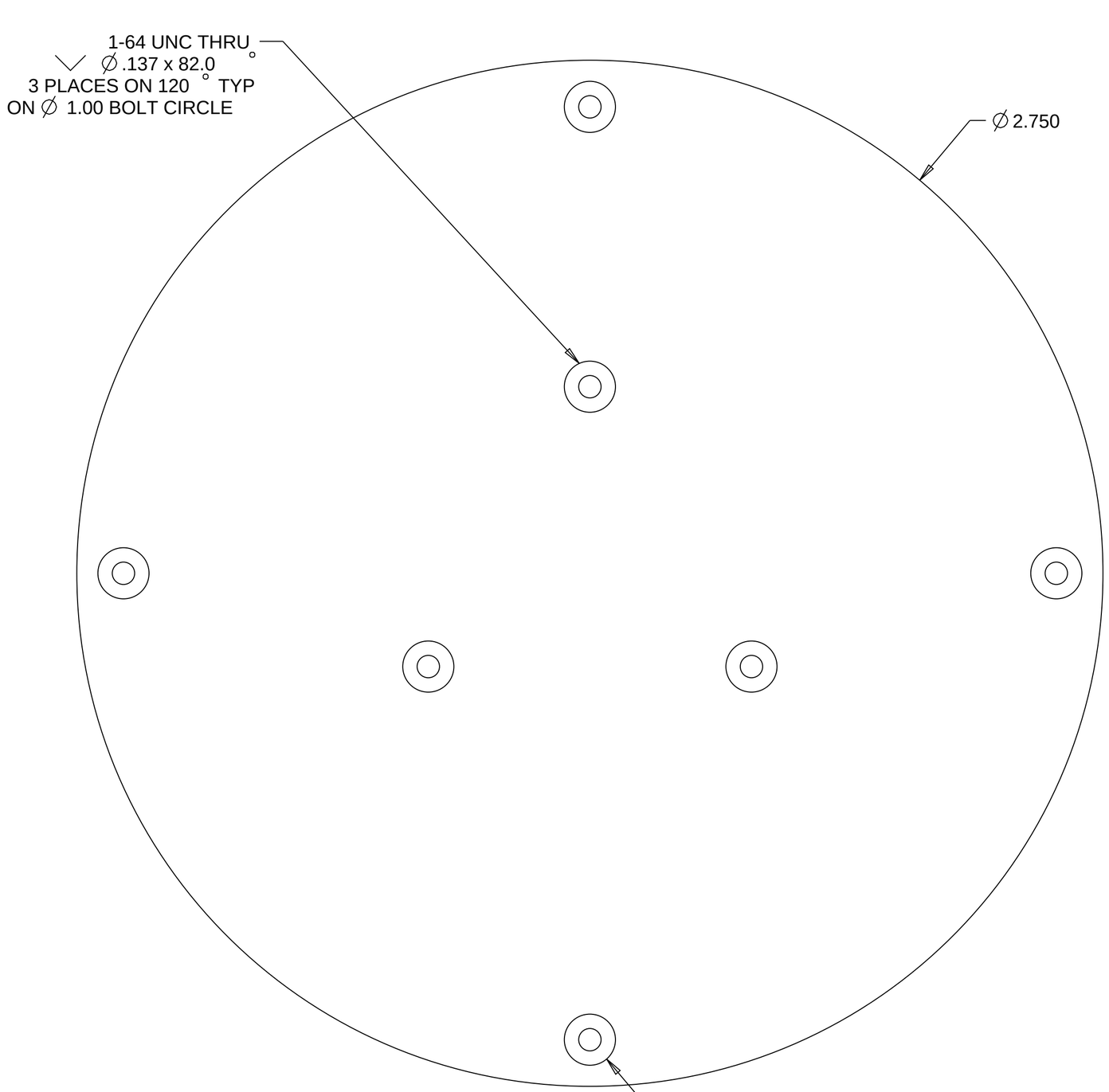


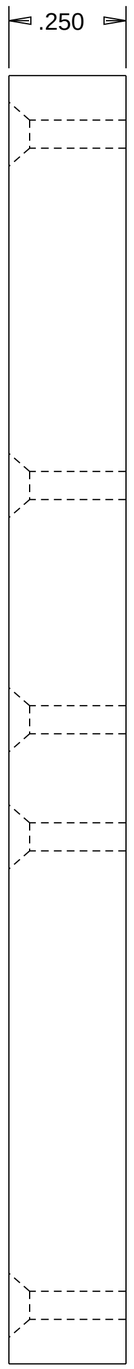


| | |
|---|---|
| Part: | Bottom Housing |
| Project: | Rotary Actuator |
| Drawn by: | Group 9 |
| Date: | 11/30/2007 |
| Sheet: | 5 of 16 |
| Sandia National Laboratory | |
| FAMU-FSU College of Engineering | |

SCALE 4.000

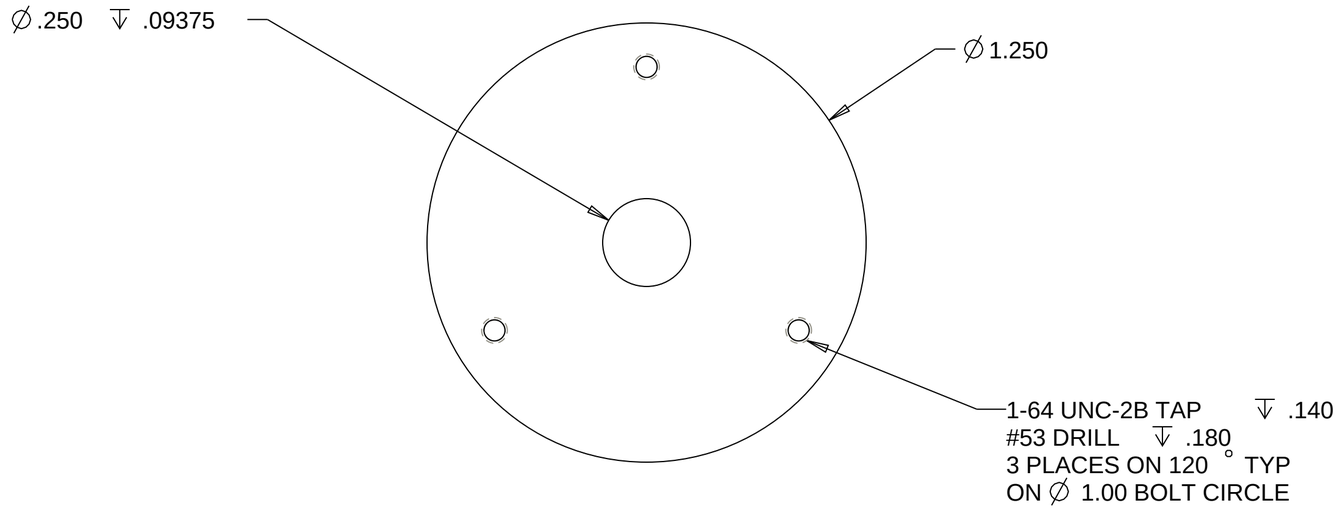


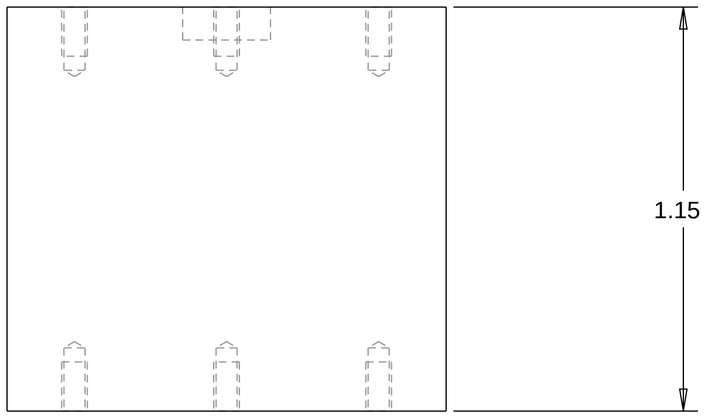


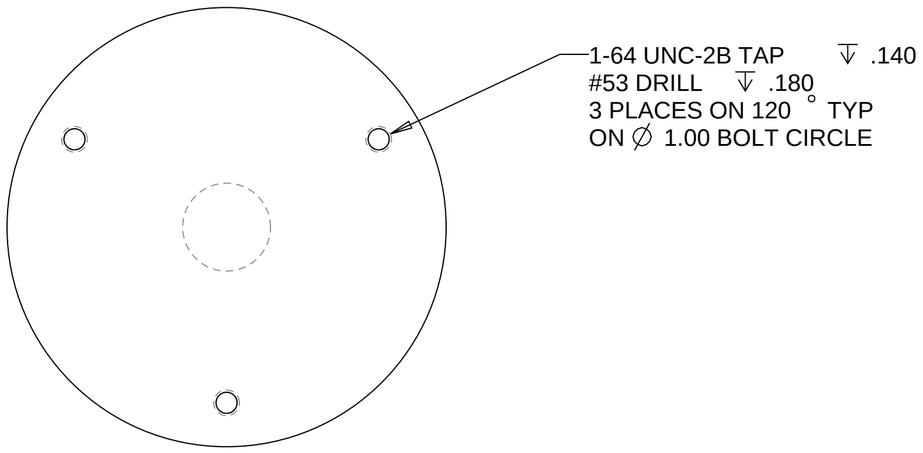


| | |
|---|---|
| Part: | Steel Rod |
| Project: | Rotary Actuator |
| Drawn by: | Group 9 |
| Date: | 11/30/2007 |
| Sheet: | 6 of 16 |
| Sandia National Laboratory | |
| FAMU-FSU College of Engineering | |

SCALE 3.000

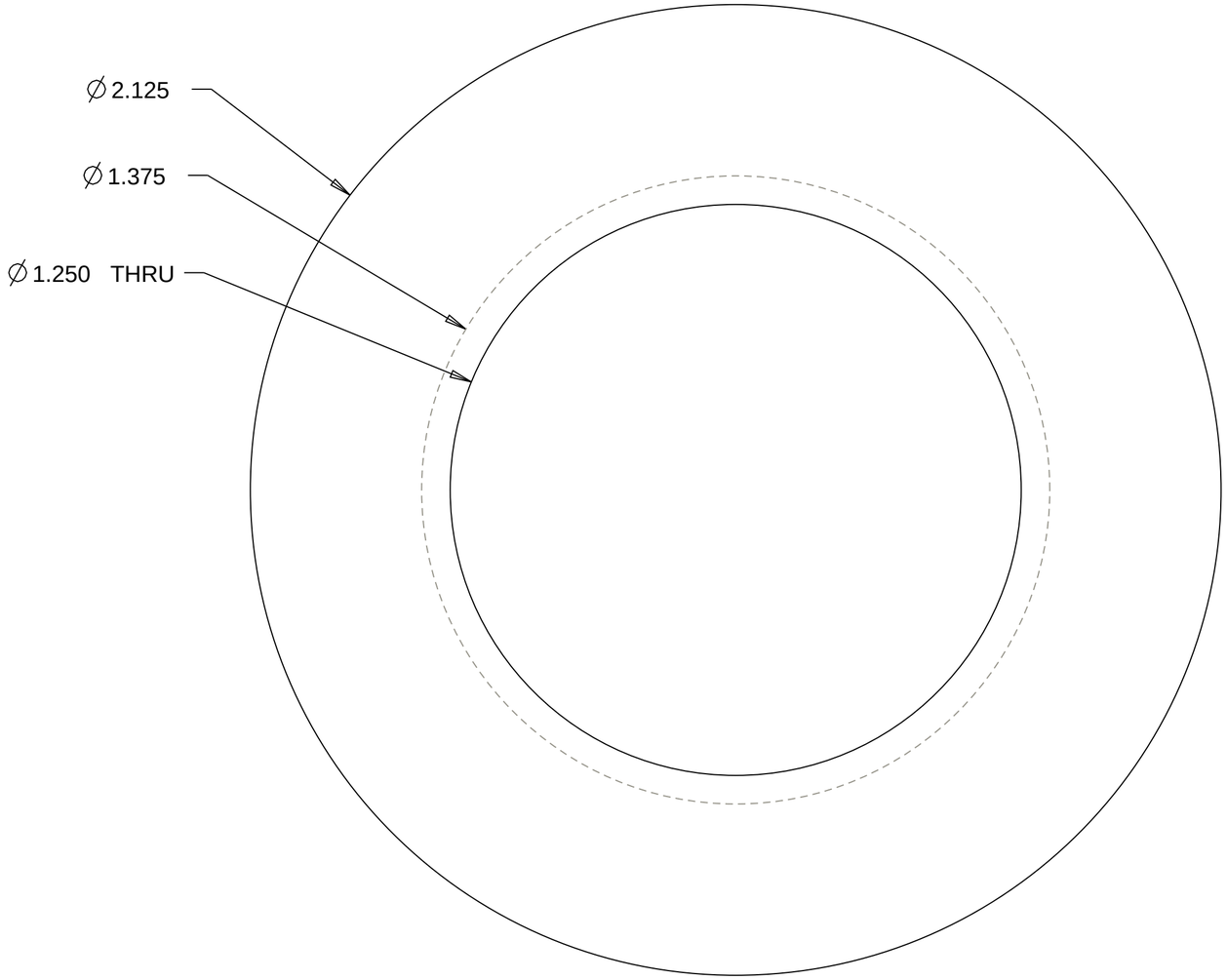


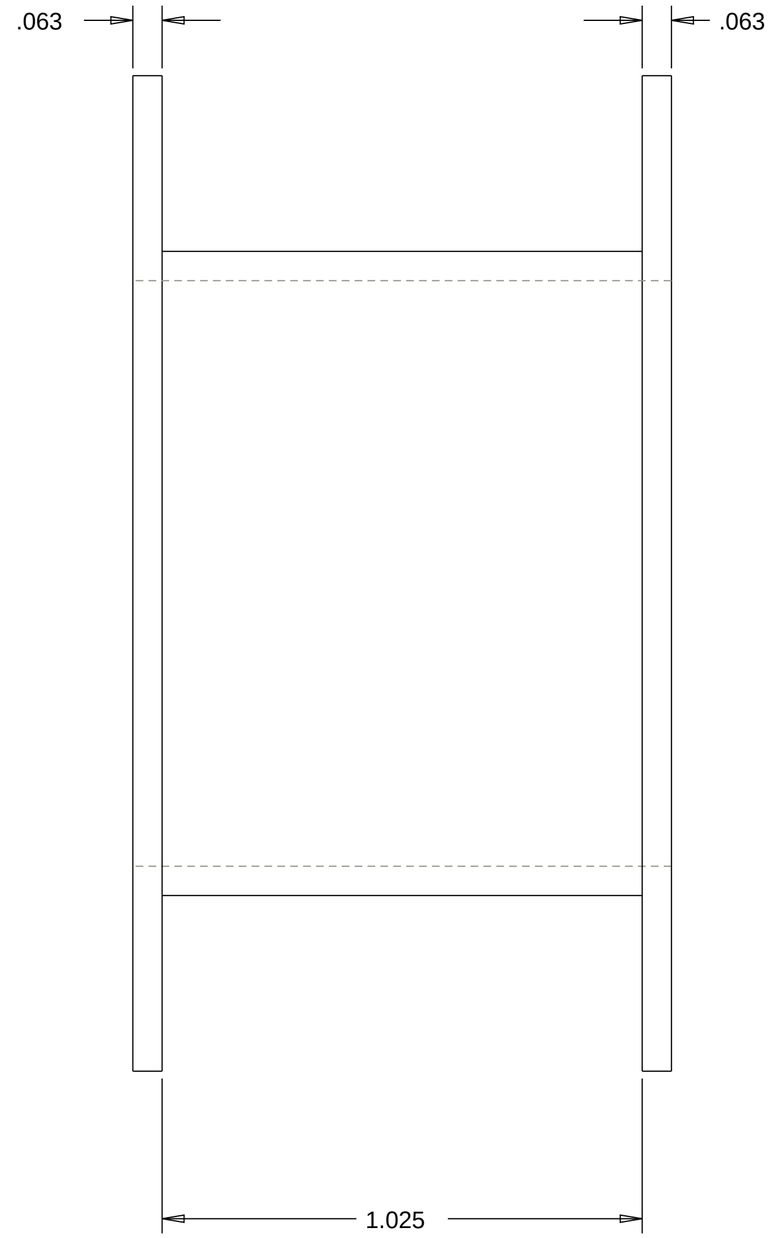


| | |
|---|---|
| Part: | Coil Spool |
| Project: | Rotary Actuator |
| Drawn by: | Group 9 |
| Date: | 11/30/2007 |
| Sheet: | 7 of 16 |
| Sandia National Laboratory | |
| FAMU-FSU College of Engineering | |

SCALE 4.000

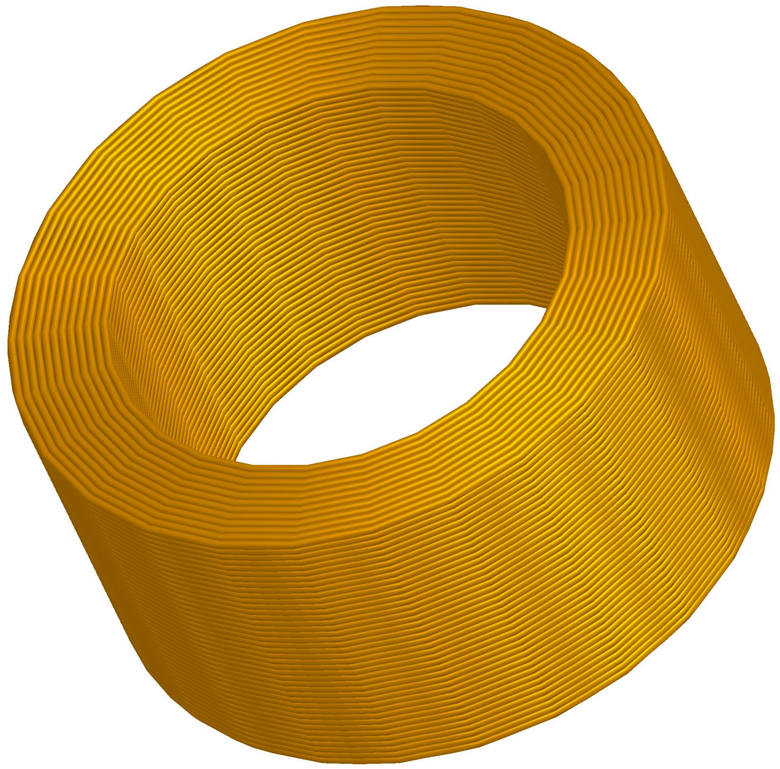

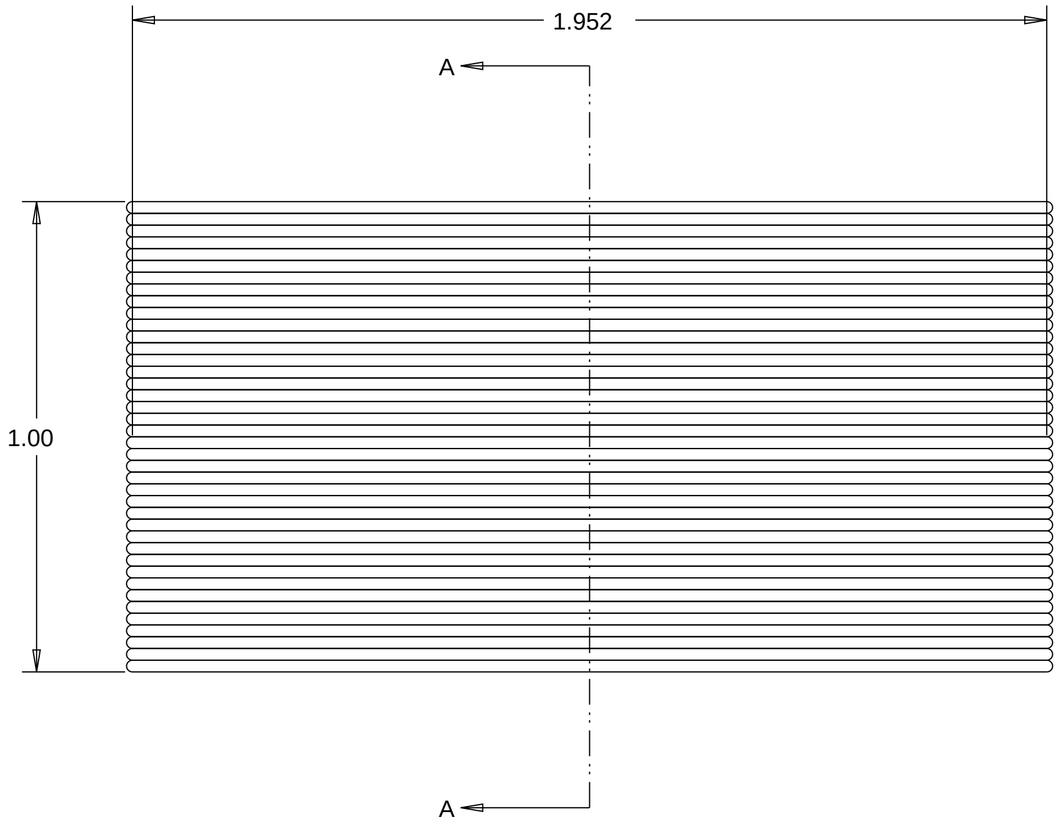


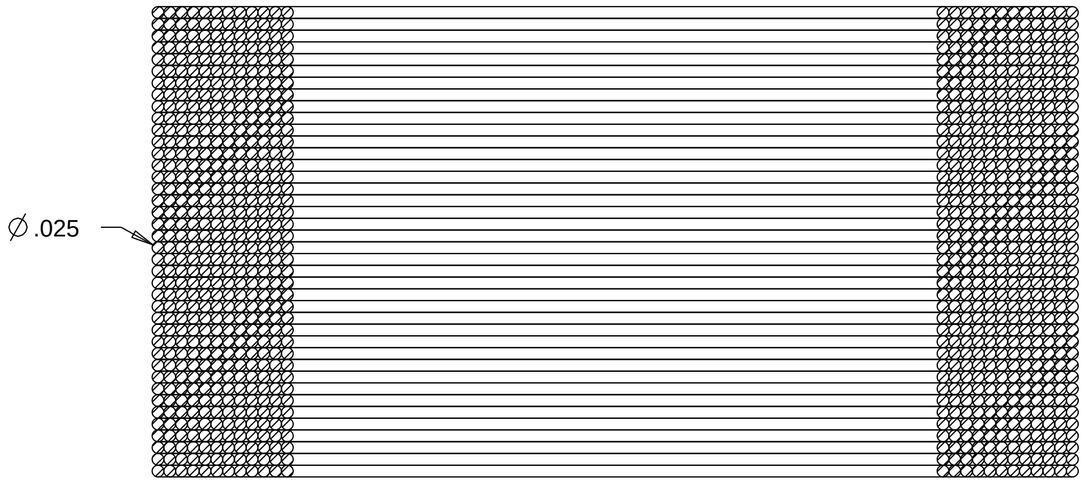


SECTION A-A

SCALE 4.000

| | |
|---|---|
| Part: | Coil |
| Project: | Rotary Actuator |
| Drawn by: | Group 9 |
| Date: | 11/30/2007 |
| Sheet: | 8 of 16 |
| Sandia National Laboratory | |
| FAMU-FSU College of Engineering | |

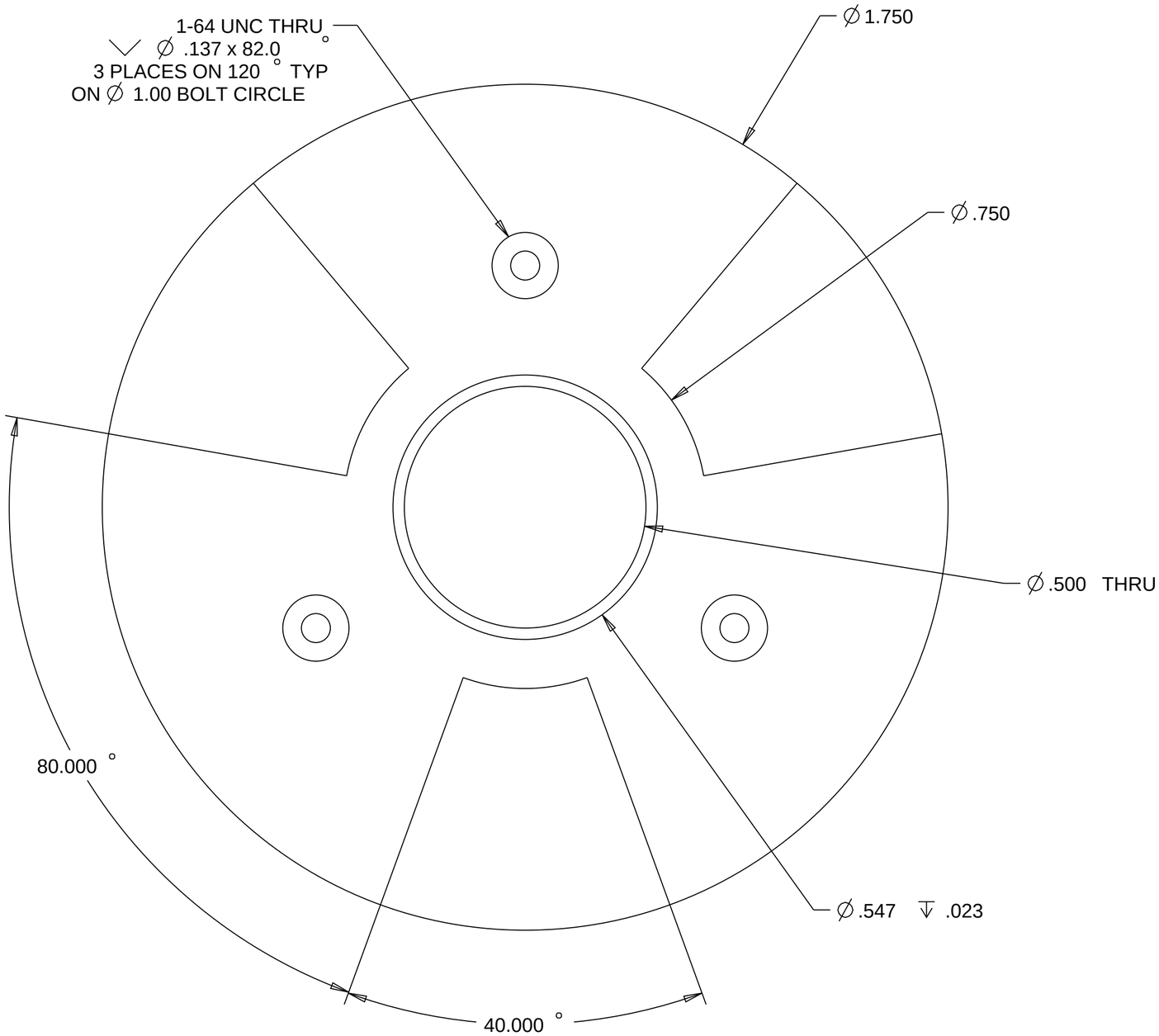


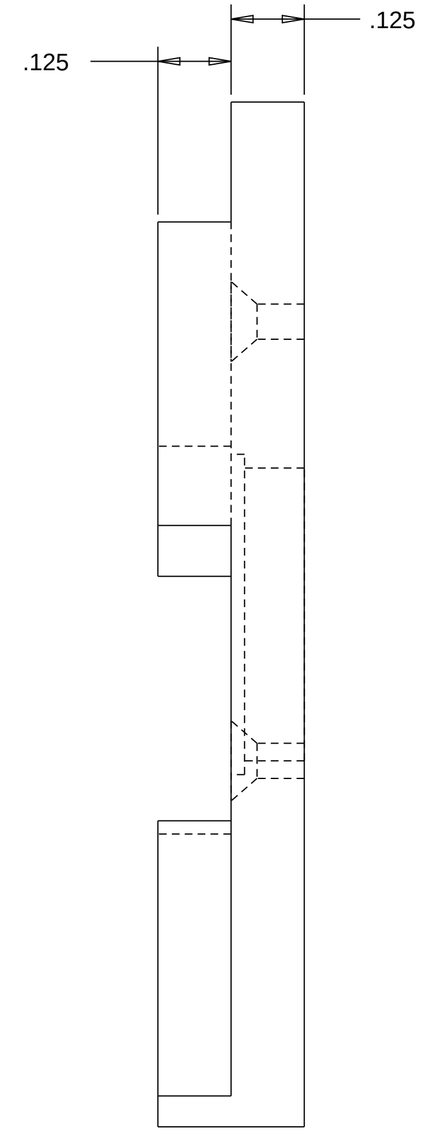


| | |
|---|---|
| Part: | Lower Stator |
| Project: | Rotary Actuator |
| Drawn by: | Group 9 |
| Date: | 11/30/2007 |
| Sheet: | 9 of 16 |
| Sandia National Laboratory | |
| FAMU-FSU College of Engineering | |

SCALE 5.000

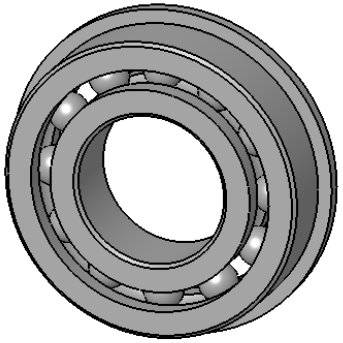

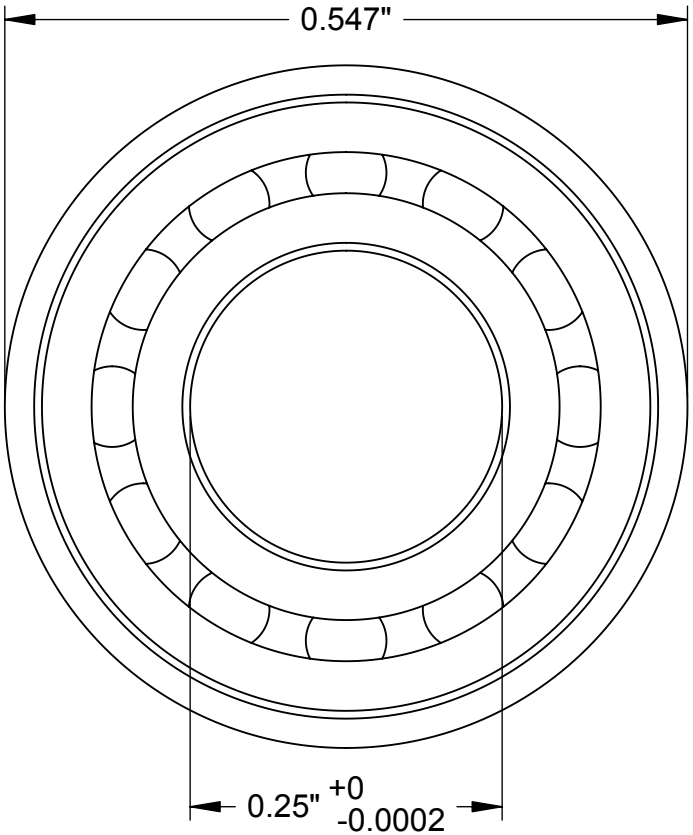


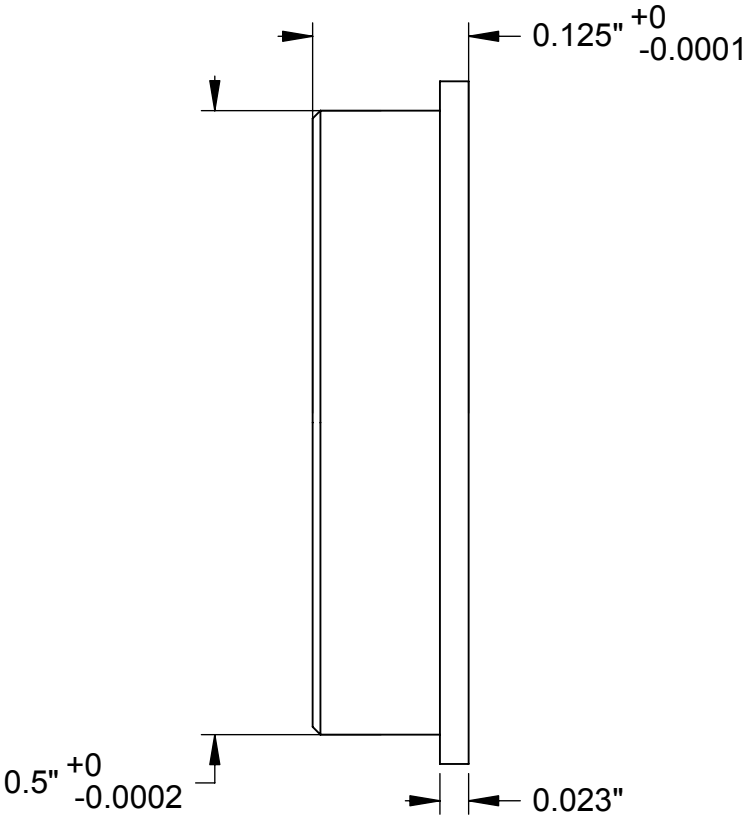


McMASTER-CARR CAD

PART NUMBER **4259T15**

http://www.mcmaster.com



Type 440C Stainless Steel Flanged Open Ball Bearing

Unless otherwise specified, dimensions are in inches. Information in this drawing is provided for reference only.

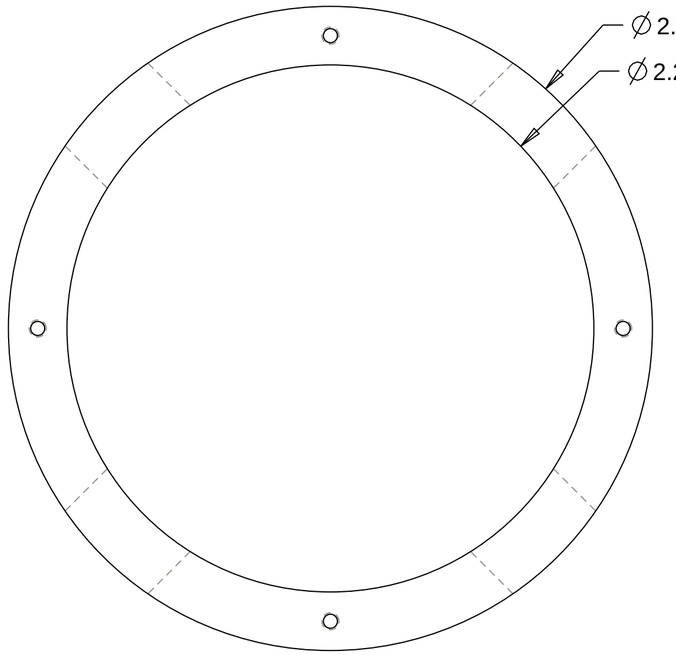


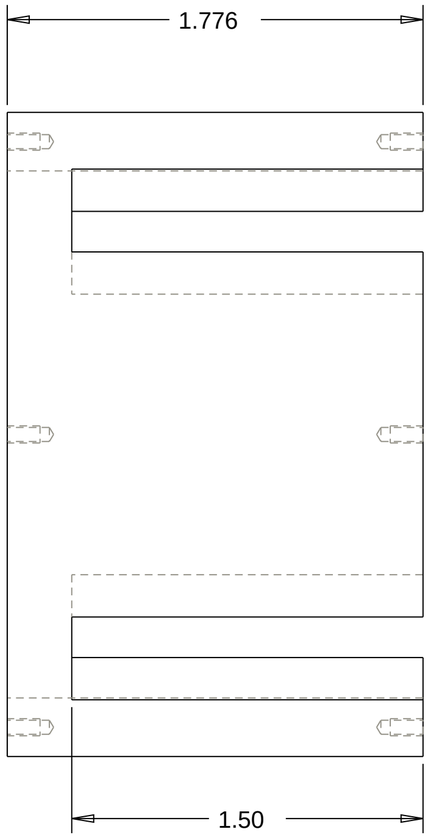


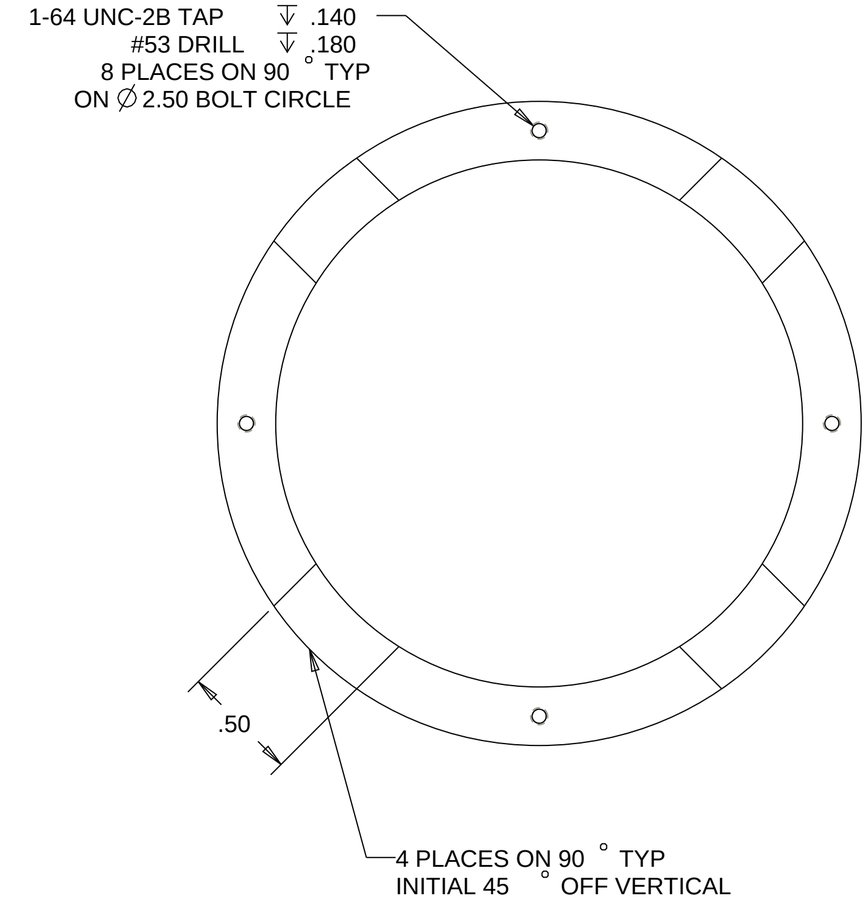


| | |
|---|---|
| Part: | Outer Structure |
| Project: | Rotary Actuator |
| Drawn by: | Group 9 |
| Date: | 11/30/2007 |
| Sheet: | 11 of 16 |
| Sandia National Laboratory | |
| FAMU-FSU College of Engineering | |

SCALE 2.000

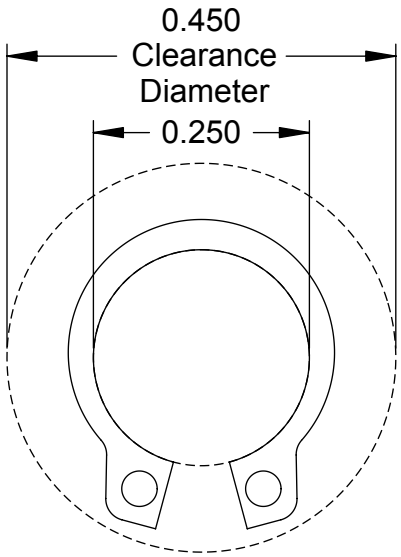


Expanded over Shaft

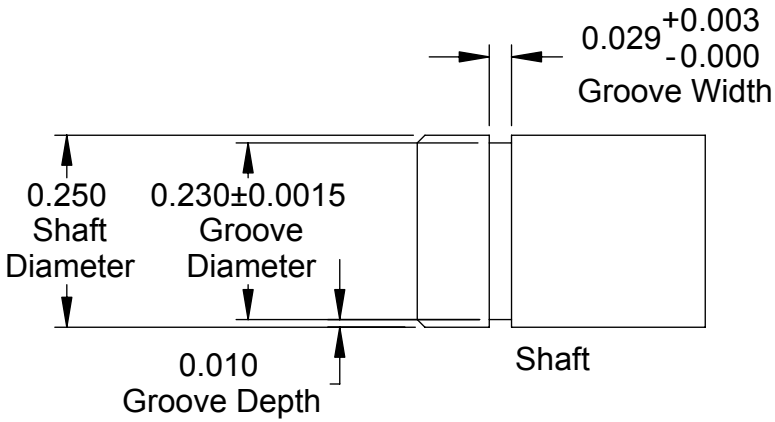


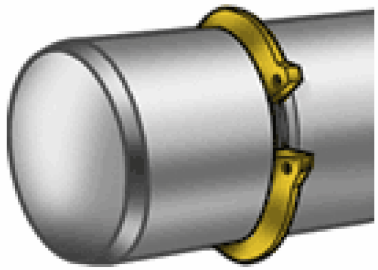

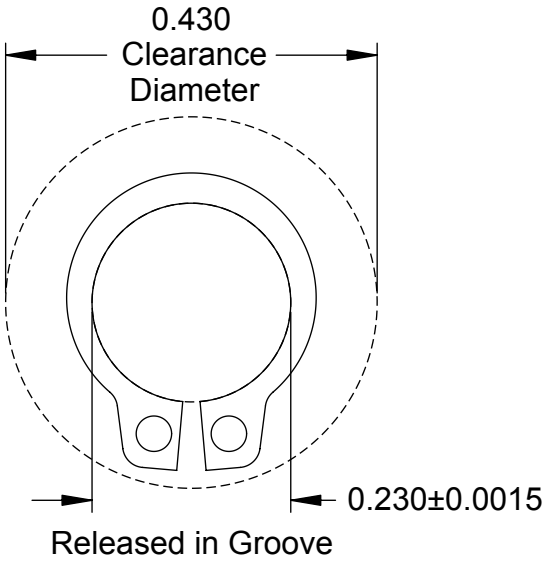


Released in Groove


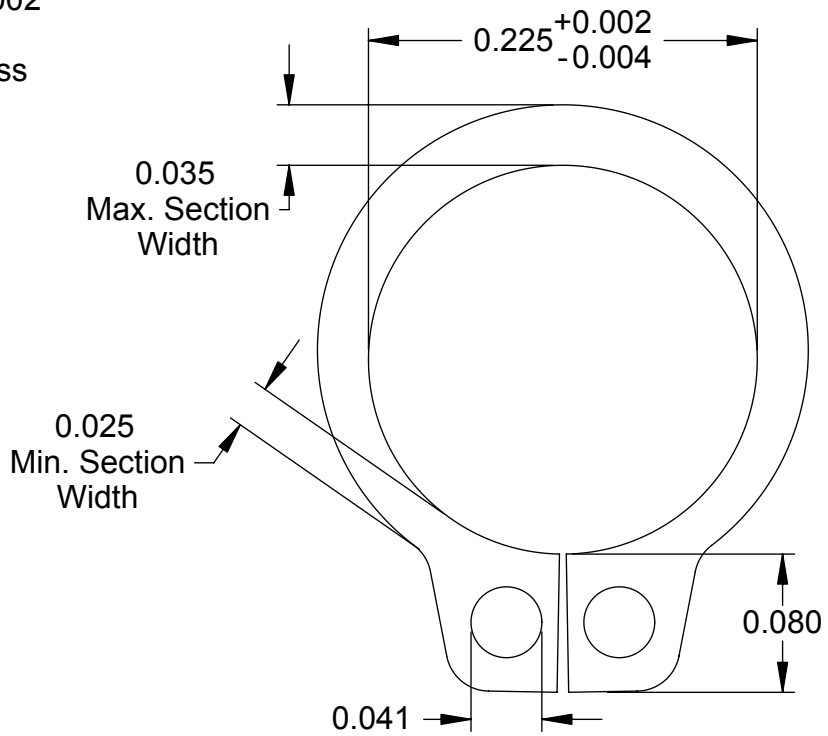


Note: Clearance diameter is the diameter of a housing that can pass freely over the ring.

McMASTER-CARR CAD

PART NUMBER **91590A113**

http://www.mcmaster.com



Stainless Steel
External Retaining Ring

Unless otherwise specified, dimensions are in inches. Information in this drawing is provided for reference only.

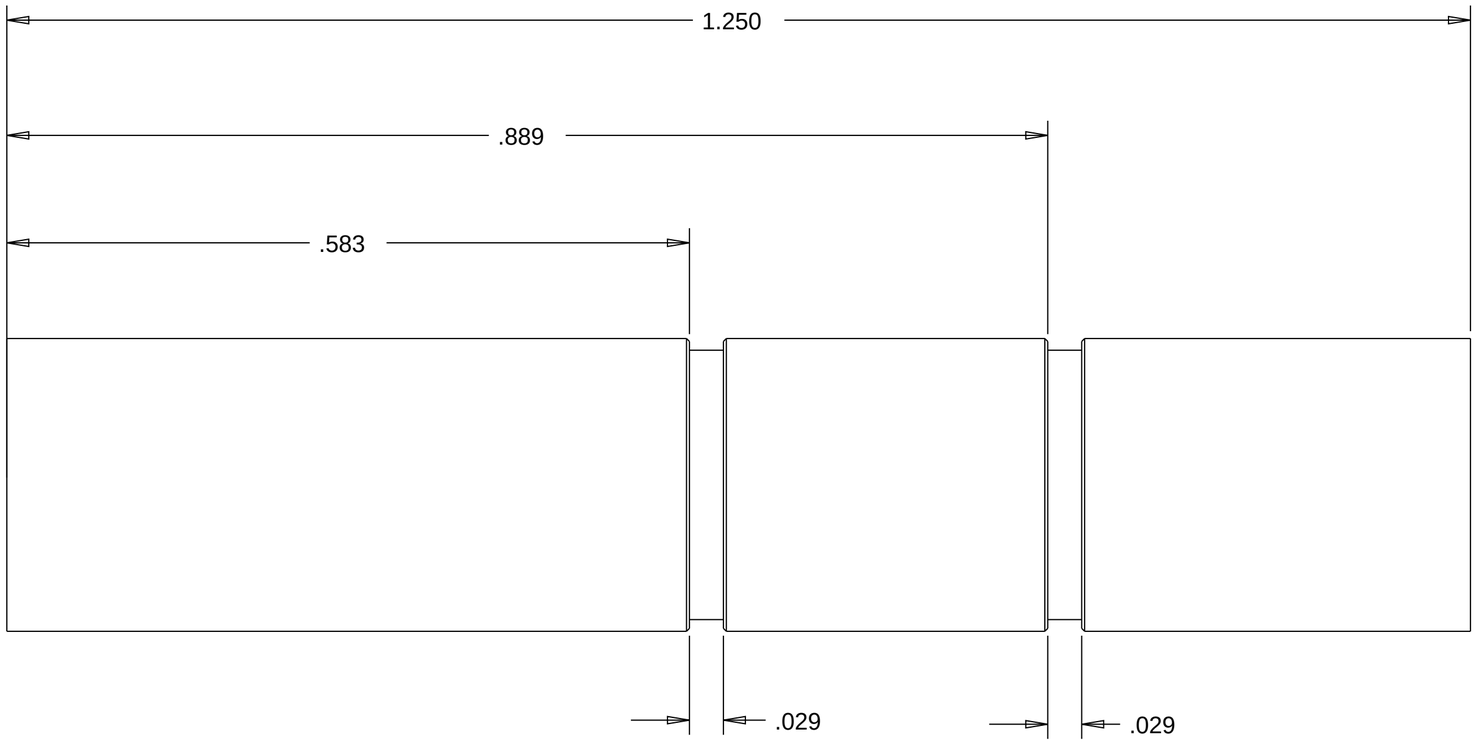


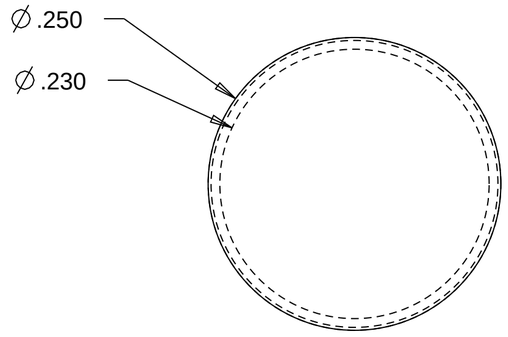


| | |
|---|---|
| Part: | Shaft |
| Project: | Rotary Actuator |
| Drawn by: | Group 9 |
| Date: | 11/30/2007 |
| Sheet: | 13 of 16 |
| Sandia National Laboratory | |
| FAMU-FSU College of Engineering | |

SCALE 10.000

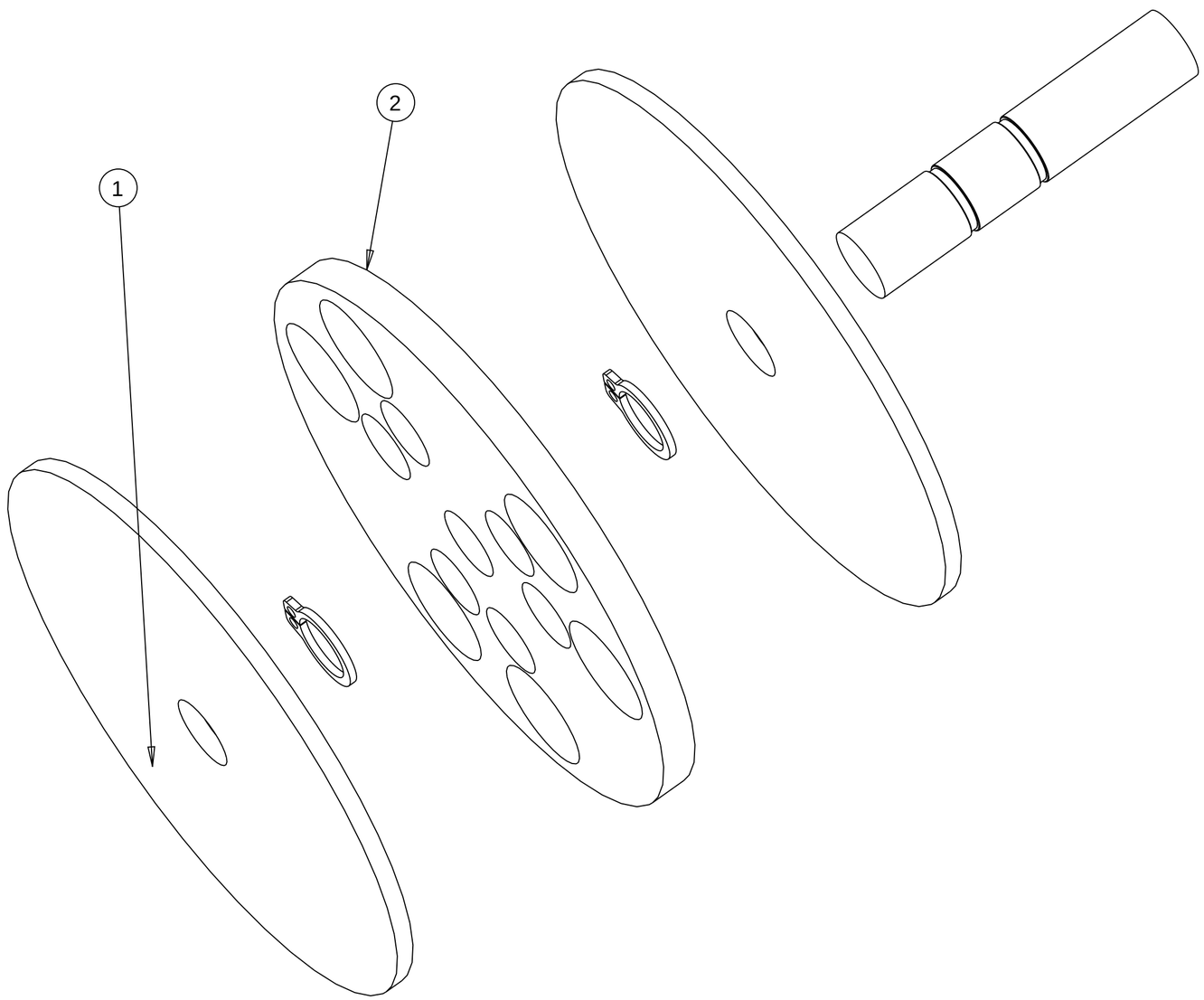


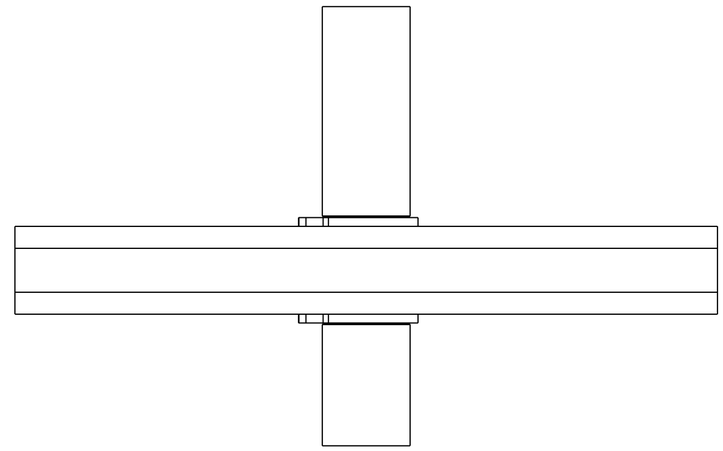

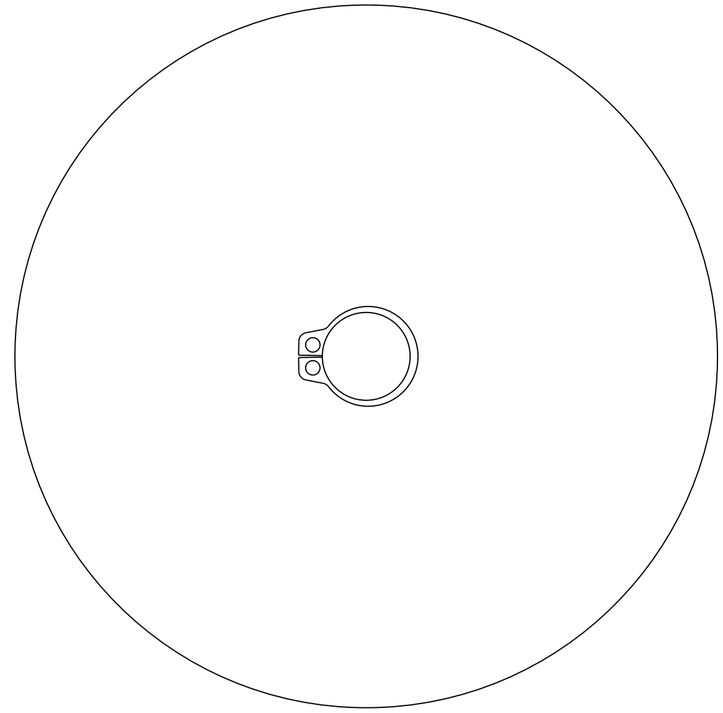

| | |
|---|---|
| Part: | Rotor Assembly |
| Project: | Rotary Actuator |
| Drawn by: | Group 9 |
| Date: | 11/30/2007 |
| Sheet: | 14a of 16 |
| Sandia National Laboratory | |
| FAMU-FSU College of Engineering | |

SCALE 3.000

Bill of Materials:

| Quantity | Part # | Name |
|---|---|---|
| 2 | 1 | ROTOR CAP |
| 1 | 2 | ROTOR CORE |

| | |
|---|---|
| Part: | Bill of Materials |
| Project: | Rotary Actuator |
| Drawn by: | Group 9 |
| Date: | 11/30/2007 |
| Sheet: | 14b of 16 |
| Sandia National Laboratory | |
| FAMU-FSU College of Engineering | |

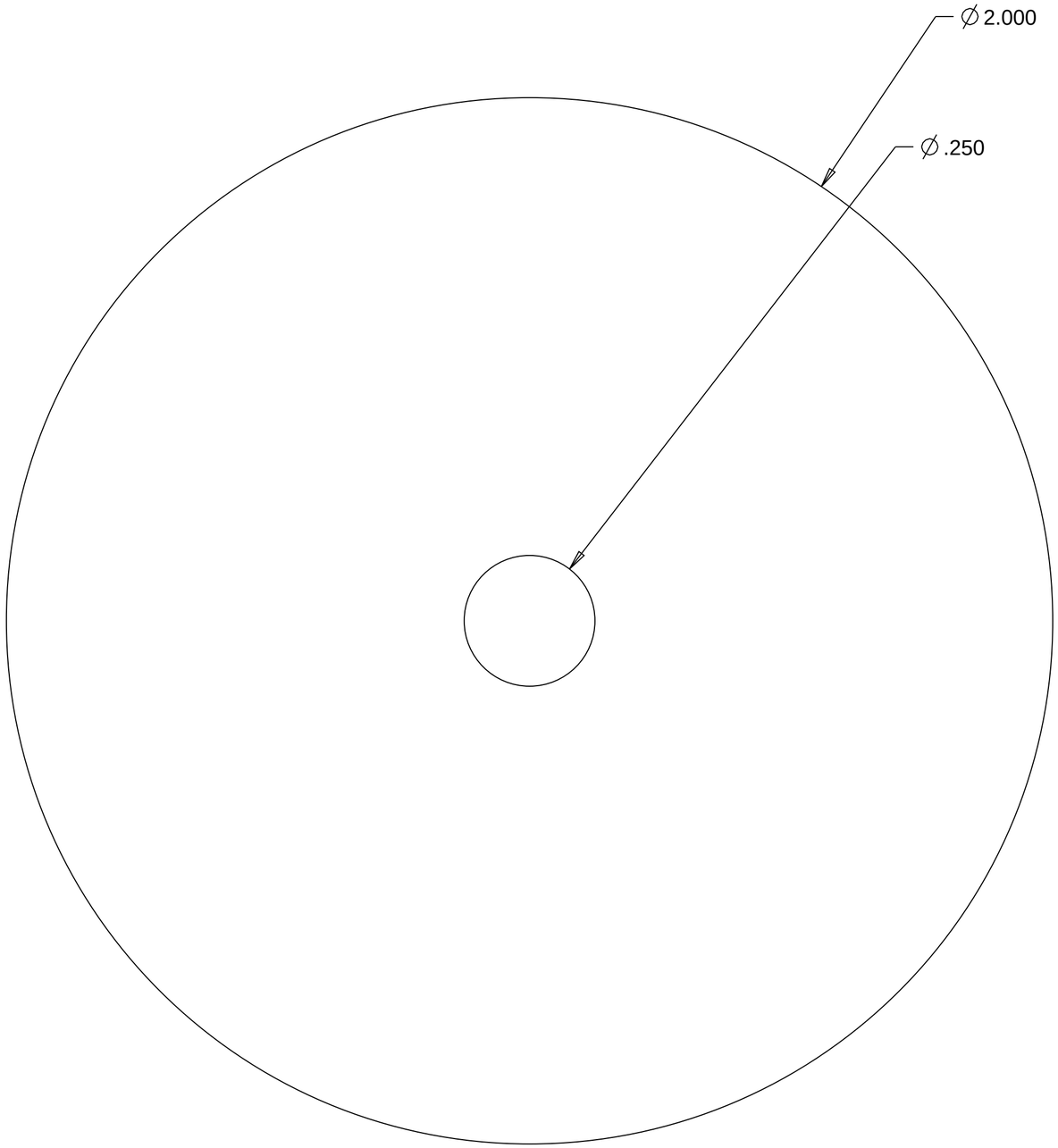


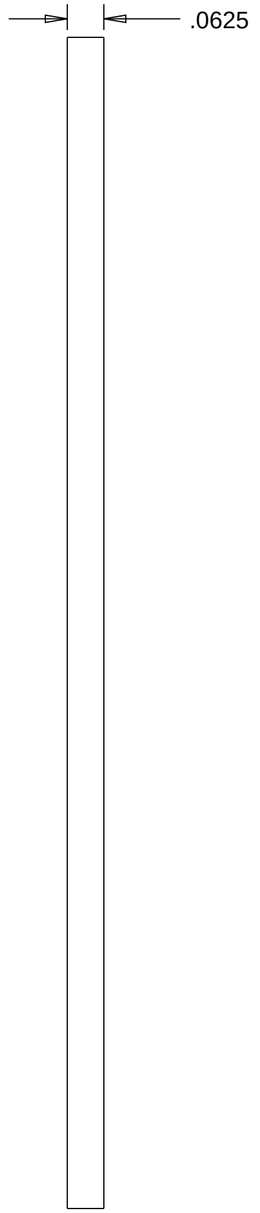


| | |
|---|---|
| Part: | Rotor Cap |
| Project: | Rotary Actuator |
| Drawn by: | Group 9 |
| Date: | 11/30/2007 |
| Sheet: | 14c of 16 |
| Sandia National Laboratory | |
| FAMU-FSU College of Engineering | |

SCALE 5.000

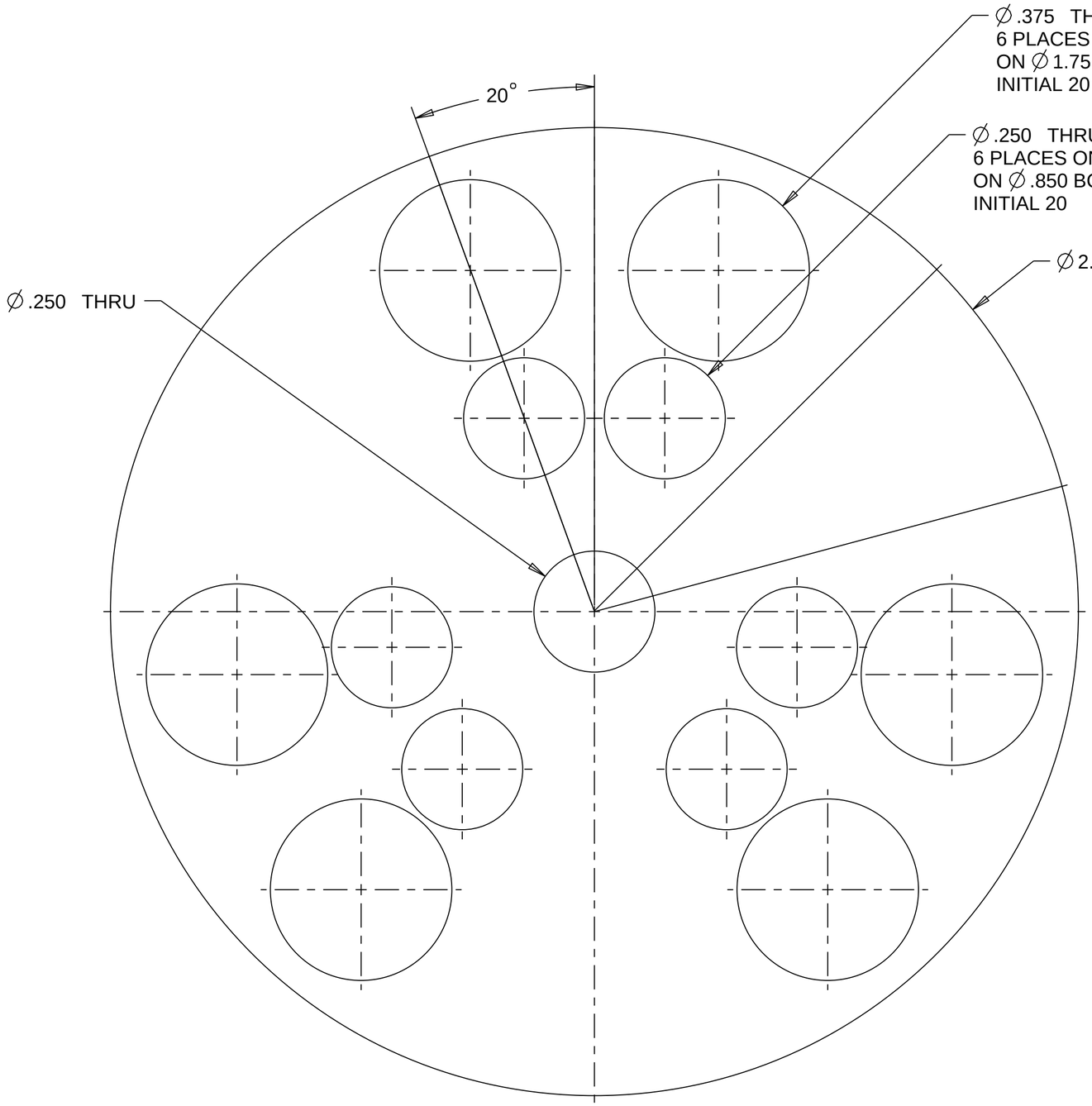


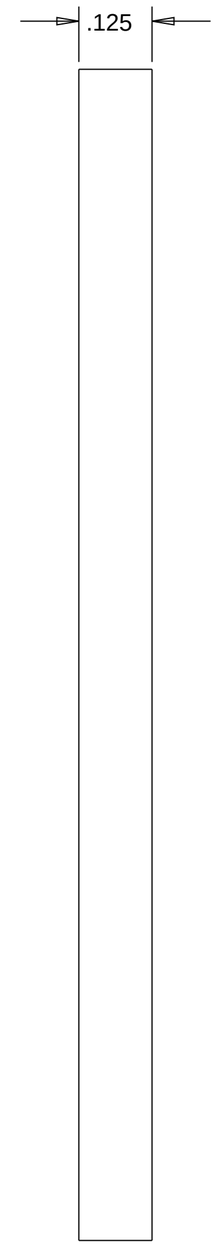


| | |
|---|---|
| Part: | Rotor Core |
| Project: | Rotary Actuator |
| Drawn by: | Group 9 |
| Date: | 11/30/2007 |
| Sheet: | 14d of 16 |
| Sandia National Laboratory | |
| FAMU-FSU College of Engineering | |

SCALE 5.000

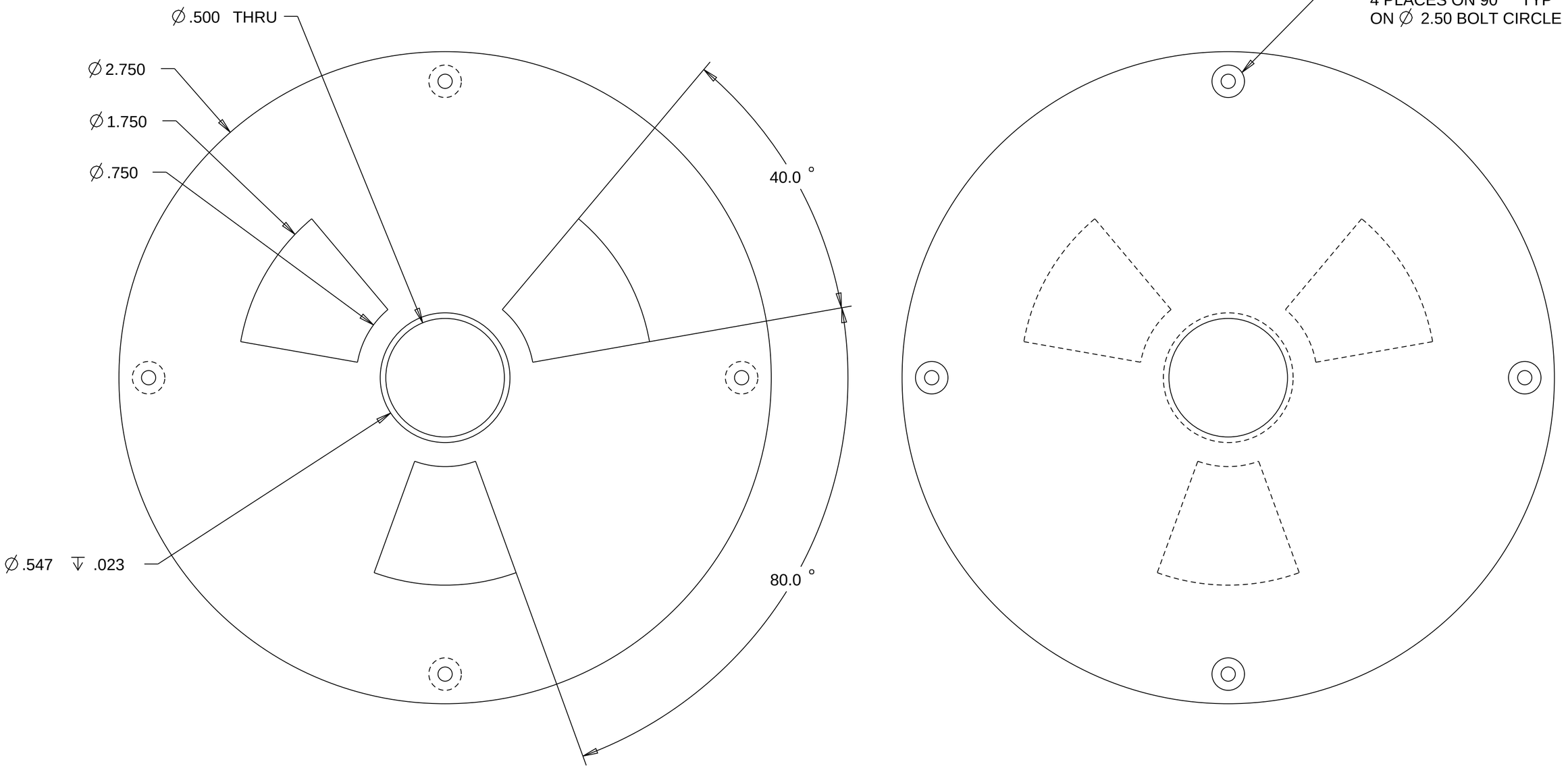


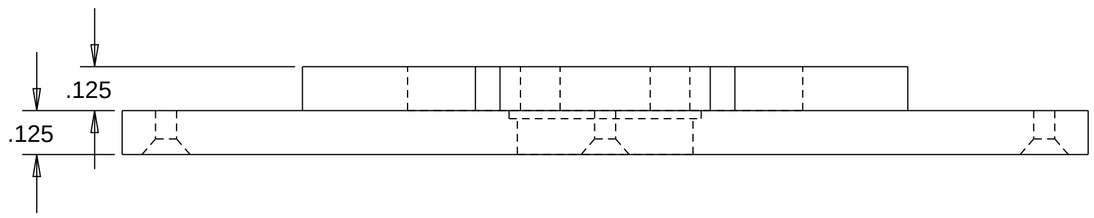


| | |
|---|---|
| Part: | Upper Stator |
| Project: | Rotary Actuator |
| Drawn by: | Group 9 |
| Date: | 11/30/2007 |
| Sheet: | 15 of 16 |
| Sandia National Laboratory | |
| FAMU-FSU College of Engineering | |

SCALE 3.000

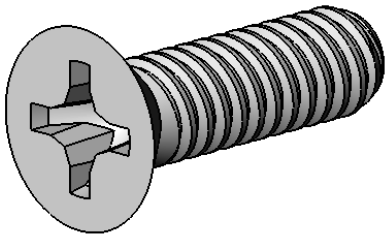

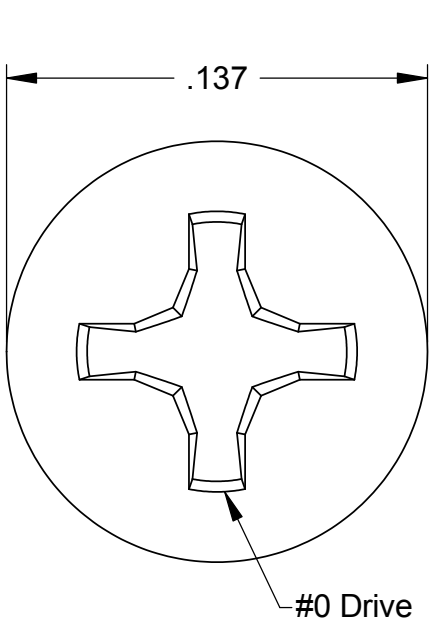


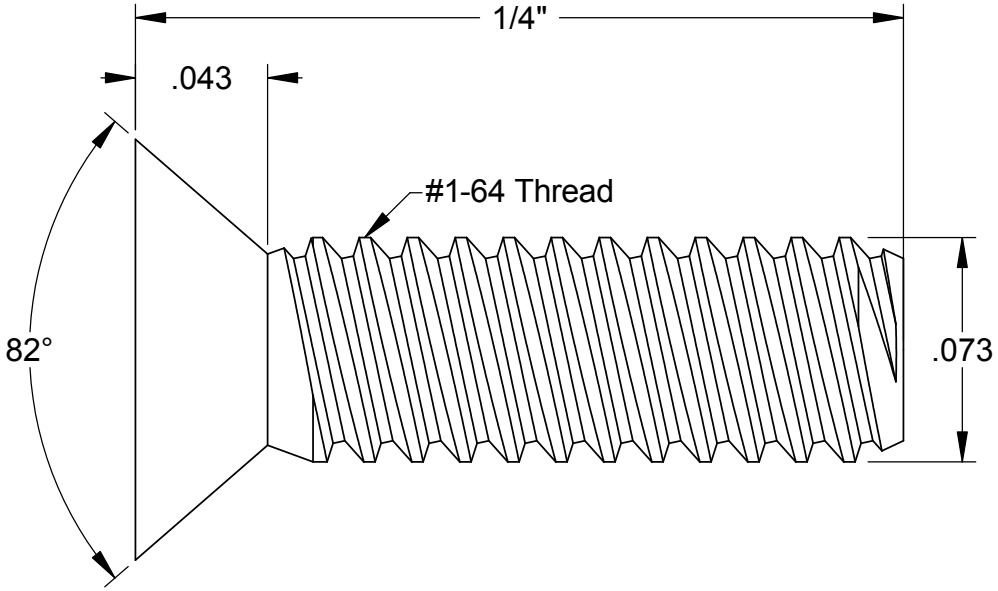


| | |
|---|---|
| McMASTER-CARR CAD | PART NUMBER **91771A066** |
| http://www.mcmaster.com<br> | 18-8 Stainless Steel Phillips Flat Head Machine Screw |

Unless otherwise specified, dimensions are in inches. Information in this drawing is provided for reference only.

# Appendix F

# Reference Papers

Library of Congress Catalog Card No. 73-647018
ISBN 0-931538-03-3
ISSN 0092-1661

Published by the Incremental Motion Control Systems Society
Post Office Box 2772, Station A, Champaign, Illinois 61820

# A DISK-ROTOR PERMANENT-MAGNET STEP MOTOR

B. C. Kuo

Department of Electrical Engineering
University of Illinois at Urbana-Champaign
Urbana, Illinois

W. H. Yeadon

Warner Electric Brake and Clutch Co.
Marengo, Illinois

## I. INTRODUCTION

The canned-type permanent-magnet (PM) step motors [1] have gained increased popularity commercially in recent years mainly due to their low cost, simplicity in construction, and light weight.

As the name implies, the housing of the canned-type PM step motor is a metal can. The stator teeth assemblies are punched out of metal sheets, and the stator windings are in the form of bobbin-wound coils. The rotor consists of a cylindrical piece of magnetic material which is magnetized with multiple numbers of poles with alternate polarities along the periphery of the rotor. Figure 1 shows the simplified cross-sectional views of the motor which has two stator sections. The teeth of one stator section are displaced from those of the other by one-half of a tooth pitch.

The stator coils are usually wound bifilar so that the motor can be driven by a unipolar driver as a four-phase motor, or, the bifilar windings can be so connected that the motor can be driven as a two-phase motor by a bipolar driver. Additional sections and phases can be added lengthwise to the motor to increase the torque output.

As shown in Figure 1, when one phase of the motor is energized, the magnetic flux is essentially confined to flow only within that section of the motor. Therefore, each section of the motor is essentially isolated from the other section(s) from a magnetic sense.

The purpose of this paper is to introduce a step motor that has a disk-shaped permanent-magnet rotor. The geometry, construction, principle of operation, and typical performance characteristics of the motor are presented. The analysis and computation of the magnetic circuits of the motor are given in another paper in these Proceedings.

The advantages of the disk-rotor PM motor are:

1. The motor diameter can be made smaller than a conventional cylindrical-rotor motor having similar performance characteristics.
2. Since the poles on the rotor are magnetized in the axial direction, oriented magnetic materials such as ceramic 5 or 8 may be used instead of the non-oriented materials such as ceramic 1, commonly used on cylindrical rotors with radial air gaps. The oriented material has a greater flux density which produces more torque per ampere of input current than a non-oriented material. As a result, the damping characteristics and the motor efficiency are improved.

## II. CONSTRUCTION OF THE DISK-ROTOR MOTOR

Figure 2 shows the major components of the motor with four phases and a step resolution of 7.5 degrees (48 steps/revolution). As shown in Figure 2, the major components of the motor are:

a permanent-magnet rotor
two inner-pole assemblies
two outer-pole assemblies
two bobbin-wound coils
housing.

The two sets of inner-and outer-pole assemblies are positioned on opposite sides of the disk rotor. For the 48-step-per-revolution motor illustrated, the rotor is magnetized axially with 24 alternate North-South poles. There are 12 teeth on each of the inner- and outer-pole pieces. The tooth pitch of the inner-pole piece and the outer-pole piece is twice that of the rotor assembly. The relative positions of the inner-pole and the outer-pole assemblies on opposite sides of the rotor are offset by one-half of a tooth pitch. Figure 3 shows the relative positions between the rotor poles and the stator teeth of the two stacks. The two bobbin wound coils can each be wound with a single winding

for bipolar driving, or with bifilar windings for unipolar driving.

As shown in Fig. 3, when the teeth of stack No. 1 of the stator are in alignment with the rotor poles, those of Stack No. 2 are in total misalignment. Thus, as the phase energization is switched from Stack 2 to Stack 1, the rotor will rotate one-half of a pole pitch of the rotor. The step angle of the motor is then given by

$$\theta_s = \frac{360}{2N_p} \text{ degrees} \qquad (1)$$

where $N_p$ is the number of poles on one side of the PM rotor. For the case illustrated in Figure 1, there are 24 poles on the rotor, and $\theta_s$ is 7.5 deg/step, or the step resolution is 48 steps per revolution. $N_p$ is also equal to the total number of teeth on the inner pole piece and the outer pole piece on one stack of the stator.

Figure 4 shows two simplified cross-sectional views of the disk-rotor motor for the purpose of illustrating the main flux paths. The main flux-carrying parts of the motor include the PM rotor, the inner poles, the outer poles, the hub, and the housing. The spacer, which is located at the center of the motor, is non-magnetic and divides the motor into two sections magnetically. The main flux path of the motor is described as shown in Figure 4. If we start at the surface of a North pole on stack No. 1 of the PM rotor, as shown in Figure 4, the magnetic flux will typically go through the following parts of the motor in succession:

1. North pole on the left side of the PM rotor
2. Main air gap
3. Inner pole
4. Hub
5. Air gap between hub and housing
6. Housing
7. Air gap between housing and outer pole
8. Outer pole
9. Main air gap
10. South pole on the left side of the PM rotor, adjacent to the starting North pole.

The flux then traverses the depth of the rotor and exists at the North pole on the right side of the rotor, and then the same sequence as described above takes place in stack No. 2.

From Figure 4, we can see that one important difference between this disk-rotor motor and the conventional canned-type PM motor is that the flux paths of the former encompass the entire motor even when only one phase is excited, whereas the flux paths of the latter motor are confined to only the excited phase.

The coupling of both stacks of the motor by the magnetic flux also means that the torque developed by the motor will be affected by the stator teeth on both sides of the rotor.

## III. PERFORMANCE CHARACTERISTICS

The performance characteristics of a typical disk-rotor PM step motor are presented in this section. The physical dimensions of the motor are: length = 2 in., outer diameter = 2.5 in.

The electrical properties and characteristics are:

| | | |
|---|---|---|
| Number of phases: | 4 | (bifilar wound) |
| Winding resistance: | 1.6 | ohms per phase |
| Rated current: | 1.75 | Amp. per phase |
| Inductance: | 11 | mH (0 Amp. DC at detent position) |

The single-step responses with one-phase-on and two-phase-on excitations are shown in Figures 5 and 6, respectively.

Figures 7 and 8 illustrate the static torque curves with one-phase-on and two-phase-on excitations measured under the stated conditions. Figure 9 gives the torque-speed curves of the motor.

## IV. REFERENCES

[1] Heine, Guenther, "Small PM Stepping Motors as Dedicated Control Elements in Data Processing Technology," Proceedings of the Seventh Annual Symposium on Incremental Motion Control Systems and Devices, 1978, pp. 27-36.

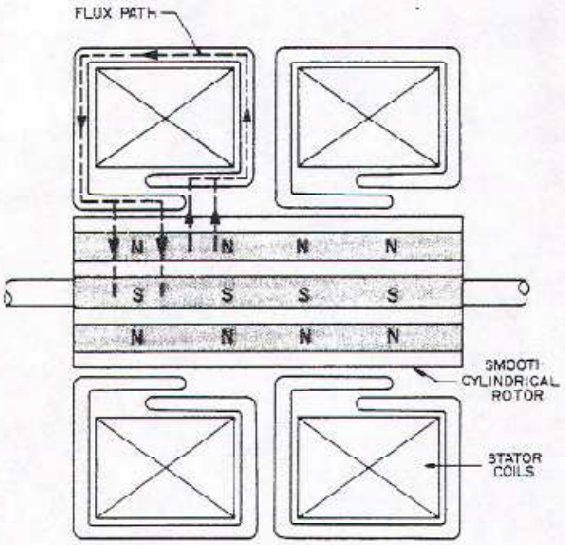


Figure 1. Cross-sectional view of the canned-type PM step motor.

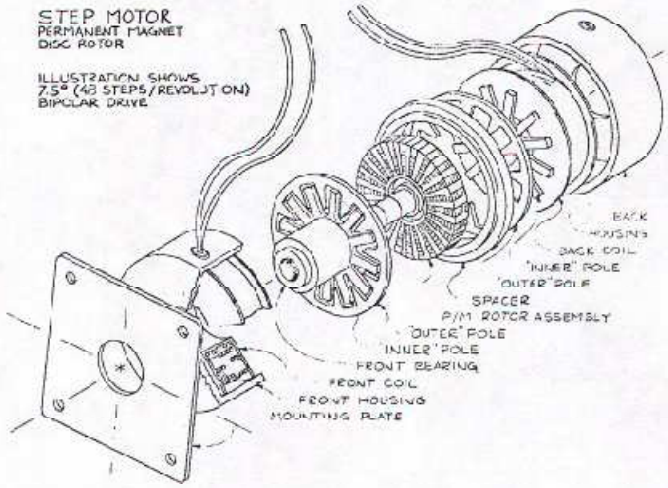


Figure 2. Principal components of the disk rotor motor.

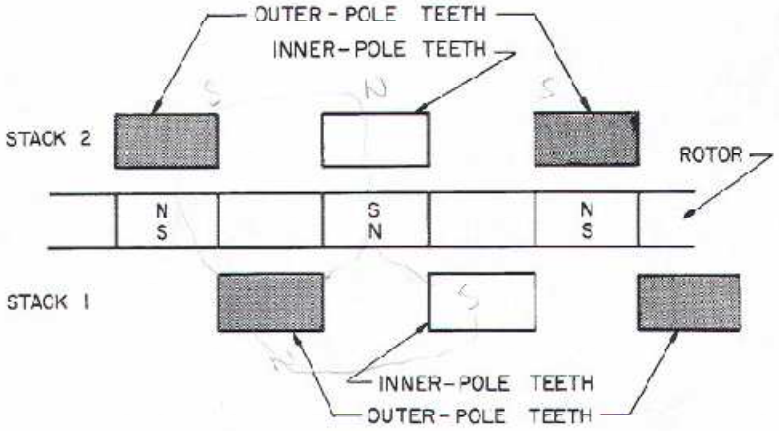


Figure 3. Inner-pole, outer-pole, and rotor relation.

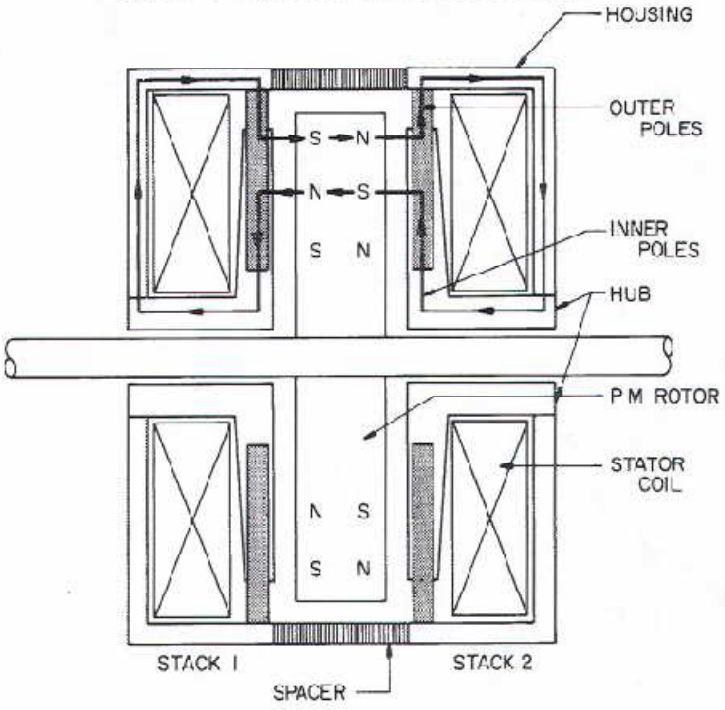


Figure 4. Cross-sectional view of the disk-rotor motor.

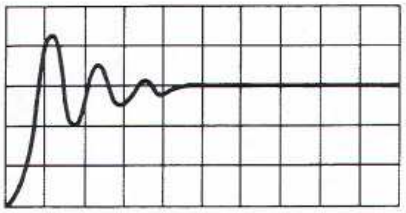

Figure 5. Single-step response.
One-phase-on excitation.
Horizontal: 10 msec/div.
Vertical: 1.25 deg/div.
30 Volts at 1.75 Amps.
8-ohm suppression.

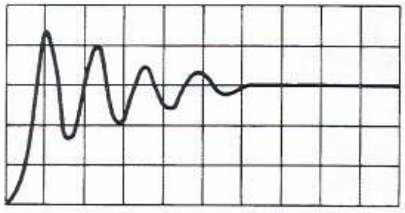

Figure 6. Single-step response.
Two-phase-on excitation.
Horizontal: 10 msec/div.
Vertical: 1.25 deg/div.
30 Volts at 1.75 Amps/phase.
8-ohm suppression.

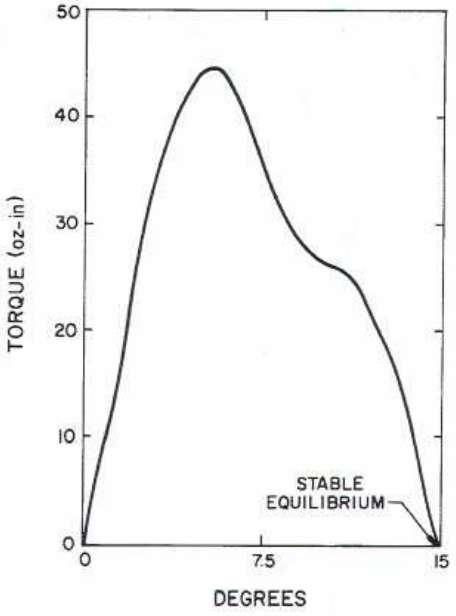


Figure 7. Static holding torque - one-phase-on.

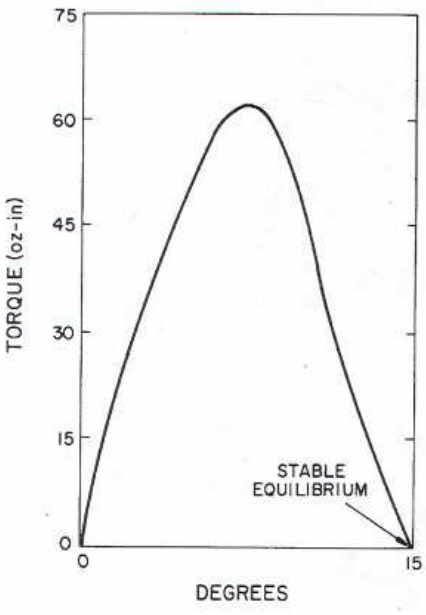


Figure 8. Static holding torque - two-phase-on.

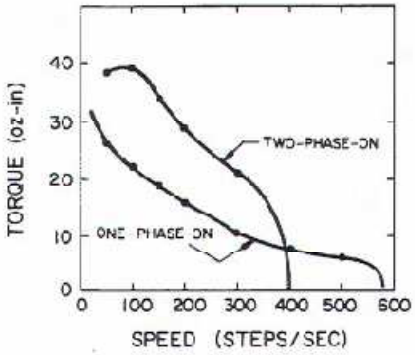


Figure 9. Torque-speed curves.

# Ultimag® Size 4EM

Part Number: 199172-0XX

All catalogue products manufactured after April 1, 2006 are RoHS Compliant

## Specifications

| | |
|---|---|
| Dielectric Strength | 1000 VRMS (23 awg); 1200 VRMS (24-33 awg) |
| Recommended Minimum Heat Sink | Maximum watts dissipated by the Ultimag are based on an unrestricted flow of air at 20°C, with the Ultimag mounted on the equivalent of an aluminium plate measuring 15.9 cm square x 0.32 cm thick |
| Thermal Resistance | 7.6°C/watt with heatsink ;<br>15.0°C/watt without heatsink |
| Rotor Inertia | $8.43 \times 10^{-7}$ (kgm²) |
| Peak Torque Rating (Tp) | 0.32 Nm |
| Power Input | 145 watts (stalled at Tp; 25°C; Pp) |
| Number of Phases | 1 |
| Static Friction (Tf) | 7 mNm |
| -3dB Closed Loop | 78 Hz |
| Maximum Winding | 180°C |
| Number of Poles | 6 |
| Weight: | 215 gms |
| Dimensions: | Ø41.66 mm x 26.3 mm L<br>(See page B10) |

## Performance

| Maximum Duty Cycle | 100% | 50% | 25% | 10% |
|---|---|---|---|---|
| $K_M$ (mNm/√watt) | 40.6 | 35.7 | 32.2 | 30.1 |
| Maximum ON Time (sec) when pulsed continuously[2] | ∞ | 40 | 15 | 4 |
| Maximum ON Time (sec) for single pulse[2] | ∞ | 108 | 34 | 9 |
| Typical Energise Time (msec)[3] | 6 | 5 | 4.5 | 3.5 |
| Watts (@ 20°C) | 14.5 | 29 | 58 | 145 |
| Ampere Turns (@ 20°C) | 510 | 721 | 1020 | 1613 |

### Coil Data

| awg (0XX)[4] | Resistance (@20°C) | # Turns[5] | VDC (Nom) | VDC (Nom) | VDC (Nom) | VDC (Nom) |
|---|---|---|---|---|---|---|
| 23 | 0.71 | 104 | 3.2 | 4.5 | 6.4 | 10.1 |
| 24 | 1.54 | 174 | 4.7 | 6.7 | 9.4 | 14.9 |
| 25 | 2.15 | 195 | 5.6 | 7.9 | 11.2 | 17.6 |
| 26 | 3.01 | 219 | 6.6 | 9.3 | 13.2 | 20.9 |
| 27 | 5.78 | 328 | 9.2 | 12.9 | 18.3 | 28.9 |
| 28 | 8.09 | 368 | 10.8 | 15.3 | 21.7 | 34.3 |
| 29 | 14.40 | 515 | 14.5 | 20.4 | 28.9 | 45.7 |
| 30 | 20.11 | 575 | 18.9 | 24.2 | 37.7 | 59.6 |
| 31 | 34.40 | 774 | 22.3 | 31.6 | 44.6 | 71.0 |
| 32 | 56.60 | 1009 | 28.7 | 40.5 | 57.0 | 91.0 |
| 33 | 91.40 | 1288 | 36.0 | 51.5 | 73.0 | 115.0 |

## How to Order

Add the coil awg number (0XX) to the part number (for example: to order a 25% duty cycle rated at 18.5 VDC, specify 100172-027).

Please see www.ledex.com (click on Stock Products tab) for our list of stock products available through our distributors.

[1] Continuously pulsed at stated watts and duty cycle

[2] Single pulse at stated watts (with coil at ambient room temperature 20°C)

[3] Typical energise time based on no load condition. Times shown are for half of full rotary stroke starting at centre-off position.

[4] Other coil awg sizes available — please consult factory

[5] Reference number of turns

WARNING: Exposed Magnet may affect pacemakers.
In the event a product unit's magnet is exposed due to product disassembly, Pacemaker Wearers should distance themselves 3 metres from exposed magnet.

All specifications subject to change without notice.

# References

Society., Incremental. 1981. Incremental Motion Control Systems and Devices: Proceedings, Tenth Annual Symposium, June, 1981. Champaign, Ill. Incremental Motion Control Systems Society.

Motor Engineering. Chatsworth: NMB Technologies Coporation. Accessed December 1 2007, from: <nmbtc.com>.

Condit, Reston. 2004. "Stepping Motor Fundamentals." [Available Online] [cited December 1, 2007] Available from www.microchip.com.

Solenoid Basic. Vandalia. Accessed December 1 2007, from: <www.ledex.com>.

Lazic, Anita, Browning, Bert, Nwabude, Tiffany, and Fallen, Tio. 2006. Axial Flux Permanent Magnet Micromotor Based on MEMS Technology. Thesis, Engineering, Florida State University, Tallahassee.